

---

# COMBINATORIAL GAUSSIAN PROCESS BANDITS IN BAYESIAN SETTINGS: THEORY AND APPLICATION FOR ENERGY-EFFICIENT NAVIGATION

---

**Jack Sandberg**  
Chalmers University of Technology  
Gothenburg, Sweden  
jack.sandberg@chalmers.se

**Niklas Åkerblom**  
Volvo Car Corporation  
Chalmers University of Technology  
Gothenburg, Sweden  
niklas.akerblom@chalmers.se

**Morteza Haghiri Chehrehani**  
Chalmers University of Technology  
Gothenburg, Sweden  
morteza.chehrehani@chalmers.se

## ABSTRACT

We consider a combinatorial Gaussian process semi-bandit problem with time-varying arm availability. Each round, an agent is provided a set of available base arms and must select a subset of them to maximize the long-term cumulative reward. Assuming the expected rewards are sampled from a Gaussian process (GP) over the arm space, the agent can efficiently learn. We study the Bayesian setting and provide novel Bayesian regret bounds for three GP-based algorithms: GP-UCB, Bayes-GP-UCB and GP-TS. Our bounds extend previous results for GP-UCB and GP-TS to a combinatorial setting with varying arm availability and to the best of our knowledge, we provide the first Bayesian regret bound for Bayes-GP-UCB. Time-varying arm availability encompasses other widely considered bandit problems such as contextual bandits. We formulate the online energy-efficient navigation problem as a combinatorial and contextual bandit and provide a comprehensive experimental study on synthetic and real-world road networks with detailed simulations. The contextual GP model obtains lower regret and is less dependent on the informativeness of the prior compared to the non-contextual Bayesian inference model. In addition, Thompson sampling obtains lower regret than Bayes-UCB for both the contextual and non-contextual model.

**Keywords** Multi-armed bandits · Combinatorial bandits · Contextual bandits · Gaussian processes · Energy-efficient navigation

## 1 Introduction

The multi-armed bandit (MAB) problem is a classical machine learning problem in which an agent repeatedly has to choose between a number of available actions to perform (commonly called *arms*). After selecting an arm, the agent receives a reward from an unknown (to the agent) probability distribution associated with the chosen arm. The goal of the agent is to maximize its expected cumulative reward over a certain time horizon - either finite or infinite [1, 2]. The goal can equivalently be framed as to minimize the *regret*, which is defined as the expected difference in reward between the agent's selected arms and the optimal arm. An effective agent must balance between acting greedily and trying new arms. If the agent only chooses the arms it currently believes to be best (i.e., acts *greedily*), it may fail to discover better arms. Similarly, if the agent never selects an arm more than once, it will fail to achieve a high total reward. This is often referred to as the *exploration-exploitation trade-off*.

The standard MAB problem can be too simple for many real-world applications, which has led to many extensions to more complex settings. The combinatorial MAB [3, 4, 5] considers a problem where the agent must select a subset of the available base arms, a *super arm*, in every round. The possibly very large number of super arms necessitates efficient exploration and may require solving difficult optimization problems. We consider a *semi-bandit* setting [6] where the agent observes the individual rewards of all selected base arms, and where the reward of the super arm is the sum of all base arm rewards. The semi-bandit setting provides the agent with more information every round, which simplifies the exploration.

The arms and environments in bandit applications often have some side-information (or context) that is relevant for the reward, e.g., the titles or user specifications in a news recommendation problem. In the contextual MAB [7, 8, 9, 10], before selecting an arm, the agent is provided a context vector (for the entire environment or each individual arm) that may (randomly) vary over time. The expected reward is assumed to have some correlation with the context, and by utilizing the context the agent can learn the expected rewards more efficiently.

When the set of arms or contexts is continuous, it is necessary to impose smoothness assumptions on the expected reward since the agent can only explore a countable number of arms. A common assumption is that the expected reward is either linear or Lipschitz continuous with respect to the arm or context. Within the related field of Bayesian optimization, it is common to instead assume that the expected reward is a sample from a Gaussian process (GP) over the arm or context set. For a sufficiently smooth GP, this ensures that arms which lie close in the arm space have similar expected rewards and thus that the agent can explore efficiently. Therefore, integrating Gaussian processes into bandits can yield higher sample efficiency and improved learning.

The seminal paper of Srinivas et al. [11] introduced the GP-UCB algorithm, which combines *upper confidence bounds* (UCB) with GPs for MABs with finite or compact arm sets. Srinivas et al. provided high-probability regret bounds for GP-UCB on a MAB problem with a compact arm space. Later work by Russo and Roy [12] provided Bayesian regret bounds for GP-UCB and GP-TS, a similar algorithm based on Thompson sampling [13], in the finite-arm setting with time-varying arm availability. Time-varying arm availability (often called *volatile* or *sleeping* arms) means that not all arms are available to the agent in every round. This is a general formulation that encompasses the contextual MAB and other MAB extensions. The proof framework of [12] permits consistent proofs for UCB and TS, which we make use of in this work, but the proof for the compact arm setting was only hinted to follow by discretization arguments in [12]. Recent work by Takeno et al. [14] provided an explicit proof of the Bayesian regret bounds for GP-UCB in the compact arm setting - but without time-varying arm availability.

The combinatorial *and* contextual MAB with changing arm sets (C3-MAB) incorporates both extensions and has received much interest recently [15, 16, 17, 18, 19], with applications in online advertisement [20], epidemic control [21] and base station assignment [22]. Early work by Qin et al. [15] considered C3-MABs with linear base arm rewards and finite (and fixed) base arms. Later work by Chen et al. [16] considered more general base arm rewards, which satisfy a Hölder condition with respect to the context, and a submodular total reward function. Recent work by Nika et al. [18] considered the C3-MAB with base arm rewards sampled from a GP. Nika et al. provided high probability regret bounds for a combinatorial variant of GP-UCB with an approximation oracle. The bound depends on a given sequence of contexts and, in the worst case, linearly on the maximal size of the super arms.

In this work, we present novel Bayesian regret bounds for GP-UCB and GP-TS in the combinatorial Gaussian process semi-bandit problem with time-varying arm availability. As discussed above, the contextual setting is a special case of the time-varying setting. Additionally, we present a Bayesian regret bound for a third bandit algorithm called Bayes-GP-UCB which is based on the BayesUCB algorithm of [23]. Whilst Bayes-GP-UCB was introduced by [20] for a combinatorial bandit problem, to the best of our knowledge there are no Bayesian regret bounds for Bayes-GP-UCB - even in the non-combinatorial setting. Our regret bounds are independent of the given sequence of contexts and depend sublinearly on the size of the super arms.

To demonstrate the applicability of the proposed combinatorial GP bandit algorithms to large scale problems, we perform a case study on an online energy-efficient navigation problem for electric vehicles. Electrification within the transport sector will be critical in reducing global greenhouse gas emissions, but adoption of electric vehicles is often impeded by limited capacity of vehicle batteries and poor availability of charging stations. Energy-efficient navigation is an important and low-cost tool to increase the effective range of electric vehicles. Previous work on energy-efficient navigation has focused on offline settings where either a known model is assumed [24, 25] or large-scale datasets are available [26, 27]. When the energy-consumption is unknown and no data is available, the learning algorithm must incorporate exploration of the road network. Åkerblom et al. [28] introduced a combinatorial MAB framework using Bayesian inference to learn the energy consumption on each edge. In this work, we extend the framework of Åkerblom et al. to a contextual setting and apply it to synthetic and real-world road networks. The experimental results demonstrate that the contextual GP model achieves lower regret than the Bayesian inference model and that its

---

**Algorithm 1** Framework for combinatorial semi-bandit problem with time-varying arm sets

---

**Require:** Prior agent parameters  $\theta_0$ , base arm set  $\mathcal{A}$ , super arm set  $\mathcal{S}$ , horizon  $T$ .

- 1: **for**  $t \leftarrow 1, \dots, T$  **do**
  - 2:    $\mathcal{A}_t, \mathcal{S}_t \leftarrow \text{ObserveAvailableArms}(\mathcal{A}, \mathcal{S})$
  - 3:    $\mathbf{U}_t \leftarrow \text{GetBaseArmIndices}(t, \theta_{t-1})$
  - 4:    $\mathbf{a}_t \leftarrow \text{SelectOptimalSuperArm}(\mathcal{S}_t, \mathbf{U}_t)$
  - 5:    $\mathbf{r}_t \leftarrow \text{ObserveRewards}(\mathbf{a}_t)$
  - 6:    $\theta_t \leftarrow \text{UpdateParameters}(\mathbf{a}_t, \mathbf{r}_t, \theta_{t-1})$
- 

performance is less dependent on the informativeness of the prior. Additionally, the results show that TS obtains lower regret than Bayes-UCB for the GP and Bayesian inference models.

## 2 Setup and Algorithms

In the following section, we formulate our bandit problem, introduce Gaussian process bandit algorithms and define the information gain.

### 2.1 Problem formulation

We begin by formulating the combinatorial Gaussian process semi-bandit problem with changing arm sets.

Let  $\mathcal{A} \subset \mathbb{R}^d$  denote the set of base arms in a  $d$ -dimensional space and  $\mathcal{S} = \{\mathbf{a} | \mathbf{a} \subset \mathcal{A}\} \subset 2^{\mathcal{A}}$  denote the set of feasible super arms. The expected reward for the base arms  $f(a) \sim \mathcal{GP}(\mu(a), k(a, a'))$  is assumed to be a sample from a Gaussian process with mean function  $\mu(a) : \mathcal{A} \rightarrow \mathbb{R}$  and covariance function  $k(a, a') : \mathcal{A} \times \mathcal{A} \rightarrow [0, 1]$ .

At time  $t$ , a random and finite subset of base arms  $\mathcal{A}_t \subseteq \mathcal{A}$  is available to the agent. In a combinatorial setting, the agent must select a feasible subset of base arms, a *super arm*,  $\mathbf{a}_t \in \mathcal{S}_t$  where  $\mathcal{S}_t \subset 2^{\mathcal{A}_t}$  is the set of feasible super arms. To facilitate a feasible combinatorial problem, the number of feasible super arms is finite in each round and the super arms have a maximum size  $K$  ( $|\mathbf{a}| \leq K \forall \mathbf{a} \in \mathcal{S}_t$ ). The agent observes the rewards of the selected base arms (semi-bandit feedback)  $\mathbf{r}_t = \{r_{t,a} | a \in \mathbf{a}_t\}$  where the base arm reward  $r_{t,a} = f(a) + \epsilon$  is a sum of the expected reward and i.i.d. Gaussian noise with variance  $\varsigma^2$ . In our setting, the total reward is assumed to be additive, and the agent also observes this reward at time  $t$ :  $R_t = \sum_{a \in \mathbf{a}_t} r_{t,a}$ . The total number of time steps, the horizon, is denoted by  $T$ . Let  $H_t$  denote the history  $(\mathcal{A}_1, \mathcal{S}_1, \mathbf{a}_1, \mathbf{r}_1, \dots, \mathcal{A}_{t-1}, \mathcal{S}_{t-1}, \mathbf{a}_{t-1}, \mathbf{r}_{t-1}, \mathcal{A}_t, \mathcal{S}_t)$  of past observations and the currently available arms at time  $t$ .

In this work, we are interested in minimizing the Bayesian cumulative regret which, with a horizon of  $T$ , is defined as

$$\text{BayesRegret}(T) = \mathbb{E} \left[ \sum_{t=1}^T f(\mathbf{a}_t^*) - f(\mathbf{a}_t) \right], \quad (1)$$

where  $\mathbf{a}_t^* = \arg \max_{\mathbf{a} \in \mathcal{S}_t} f(\mathbf{a})$  and  $f(\mathbf{a}) = \sum_{a \in \mathbf{a}} f(a)$ . As discussed by Russo and Roy [12], allowing stochastic arm sets permits us to consider broader sets of bandit problems, an example of particular interest to us will be contextual models.

Algorithm 1 provides a framework for the introduced bandit problem. In the framework, the agent parameters  $\theta_t$  are defined for a general agent and are not specified here. Note that the base arm indices  $\mathbf{U}_t$  may refer to upper confidence bounds or Thompson samples, depending on the algorithm used.

### 2.2 Bayesian framework for combinatorial Gaussian process bandits

A Gaussian process  $f(a) \sim \mathcal{GP}(\mu(a), k(a, a'))$  is a collection of random variables such that for any subset  $\{a_1, \dots, a_N\} \subset \mathcal{A}$  the vector  $\mathbf{f} = [f(a_1), \dots, f(a_N)]$  has a multivariate Gaussian distribution. We take a Bayesian view of the combinatorial problem and consider  $\mathcal{GP}(\mu, k)$  as a prior over the base arm rewards. GPs are very useful for defining and solving bandit problems, due to their probabilistic nature and the flexibility they provide through design of suitable kernels.

Let  $N_{t-1} = \sum_{\tau=[t-1]} |\mathbf{a}_\tau|$  denote the total number of base arms selected up to time  $t-1$  and let  $a_1, \dots, a_{N_{t-1}}$  denote the arms selected before time  $t$ . Additionally, let  $\mathbf{y} \in \mathbb{R}^{N_{t-1}}$  denote the corresponding observed base arm rewards and

$\boldsymbol{\mu} = [\mu(a_1), \dots, \mu(a_{N_{t-1}})]^\top$  denote the corresponding prior expected base arm mean rewards. Then, for any  $a \in \mathcal{A}$ , the posterior GP distribution is given by:

$$\mu_{t-1}(a) = \mu(a) + \mathbf{k}(a)^\top (\mathbf{K} + \zeta^2 I)^{-1} (\mathbf{y} - \boldsymbol{\mu})^\top \quad (2)$$

$$k_{t-1}(a, a') = k(a, a') - \mathbf{k}(a)^\top (\mathbf{K} + \zeta^2 I)^{-1} \mathbf{k}(a'), \quad (3)$$

where  $\mathbf{K} = (k(a_i, a_j))_{i,j=1}^{N_{t-1}}$  is the covariance matrix of the previously selected arms and  $\mathbf{k}(a) = [k(a, a_1), \dots, k(a, a_{N_{t-1}})]^\top$  is the covariance between  $a$  and the previously selected arms. Let  $\sigma_{t-1}(a)$  and  $\sigma_{t-1}^2(a)$  denote the posterior standard deviation and variance respectively.

In [11], Srinivas et al. introduced the GP-UCB algorithm, which selects the next arm based on an upper confidence bound. In our combinatorial setting, the GP-UCB algorithm selects a super arm as follows

$$\mathbf{a}_t = \arg \max_{\mathbf{a} \in \mathcal{S}_t} \mu_{t-1}(\mathbf{a}) + \sqrt{\beta_t} \sigma_{t-1}(\mathbf{a}), \quad (4)$$

where  $\mu_{t-1}(\mathbf{a}) = \sum_{a \in \mathbf{a}} \mu_{t-1}(a)$ ,  $\sigma_{t-1}(\mathbf{a}) = \sum_{a \in \mathbf{a}} \sigma_{t-1}(a)$  and  $\beta_t$  is a confidence parameter, typically of order  $\mathcal{O}(\log t)$ .

Kaufmann et al. [23] introduced Bayes-UCB, which selects the arm with the largest  $(1 - \eta_t)$ -quantile, where the quantile parameter  $\eta_t$  was of order  $\mathcal{O}(1/t)$ . Adapted to the combinatorial Gaussian process setting, Bayes-UCB uses the selection rule:

$$\mathbf{a}_t = \arg \max_{\mathbf{a} \in \mathcal{S}_t} \sum_{a \in \mathbf{a}} Q(1 - \eta_t, \mathcal{N}(\mu_{t-1}(a), \sigma_{t-1}^2(a))), \quad (5)$$

where  $Q(p, \lambda)$  denotes the  $p$ -quantile of the distribution  $\lambda$ . We refer to this adapted version as Bayes-GP-UCB. Note that for  $\lambda = \mathcal{N}(\mu, \sigma^2)$ , the  $p$ -quantile is given by  $Q(p, \mathcal{N}(\mu, \sigma^2)) = \mu + \sigma \sqrt{2} \operatorname{erf}^{-1}(2p - 1)$  where  $\operatorname{erf}^{-1}(\cdot)$  is the inverse of the error function. Thus, Bayes-GP-UCB can be seen as a variant of GP-UCB where  $\beta_t = 2(\operatorname{erf}^{-1}(1 - 2\eta_t))^2$ .

GP-TS [12, 29] selects the next arm randomly by using posterior sampling. If  $\hat{f}_t(a) \sim \mathcal{GP}(\mu_{t-1}, k_{t-1})$  is a sample from the posterior distribution, then GP-TS selects the super arm according to

$$\mathbf{a}_t = \arg \max_{\mathbf{a} \in \mathcal{S}_t} \hat{f}_t(\mathbf{a}), \quad (6)$$

where  $\hat{f}_t(\mathbf{a}) = \sum_{a \in \mathbf{a}} \hat{f}_t(a)$ .

### 2.3 Information gain

The regret bounds of most GP bandit algorithms depend on a parameter called the maximal information gain  $\gamma_T$  [11, 30]. The maximal information gain (MIG) describes how the uncertainty of  $f$  diminishes as the best set of sampling points  $\mathbf{a} \subset \mathcal{A}$  grows in size  $T$ . The MIG is defined using the mutual information between the observations  $\mathbf{y}_{\mathbf{a}}$  at locations  $\mathbf{a}$  and  $f$ :

$$\gamma_T := \sup_{\mathbf{a} \subset \mathcal{A}, |\mathbf{a}| \leq T} I(\mathbf{y}_{\mathbf{a}}; f), \quad (7)$$

where  $I(\mathbf{y}_{\mathbf{a}}; f) = H(\mathbf{y}_{\mathbf{a}}) - H(\mathbf{y}_{\mathbf{a}}|f)$  and  $H(\cdot)$  denotes the entropy. In most cases, we are only interested in upper bounds of  $\gamma_T$  in terms of  $T$ . Both the true value of  $\gamma_T$  and most upper bounds depend on the kernel function  $k$  defining the GP  $f$  is sampled from. Srinivas et al. [11] initially introduced bounds on  $\gamma_T$  for common kernels, such as the Matérn and RBF kernels. Later, Vakili et al. [30] presented a general method of bounding  $\gamma_T$  that utilizes the eigendecay of the kernel  $k$ . Using this method, Vakili et al. obtained improved bounds on the Matérn kernel with smoothness parameter  $\nu$ :  $\gamma_T = \mathcal{O}\left(T^{\frac{d}{2\nu+d}} \log^{\frac{2\nu}{2\nu+d}}(T)\right)$ .

## 3 Regret Analysis

Russo and Roy [12] first provided a Bayesian regret bound for GP-UCB in a non-combinatorial setting with a finite arm set. Recently, Takeno et al. [14] presented explicit proof for the Bayesian regret of GP-UCB with a compact and fixed arm set. In this section, we present novel Bayesian regret bounds for GP-UCB and GP-TS in a combinatorial setting with time-varying arm availability. Additionally, to the best of our knowledge, we present the first Bayesian regret bound for Bayes-GP-UCB.

Similar to [11], we initially consider the finite arm case,  $|\mathcal{A}| < \infty$ , and then apply the finite arm results to a discretization. The results for the finite case are presented in Appendix B, and in this section we present the results for the infinite case.

As is common in the literature, we utilize some regularity assumptions:

**Assumption 1** (Regularity assumptions). *Assume  $\mathcal{A} \subset [0, C_1]^d$  is a compact and convex set for some  $C_1 > 0$ . Furthermore, assume that  $\mu$  and  $k$  are both  $L$ -Lipschitz on  $\mathcal{A}$  and  $\mathcal{A} \times \mathcal{A}$ , respectively, for some  $L > 0$ . In addition, for  $f \sim \mathcal{GP}(\mu, k)$  assume that there exists constants  $C_2, C_3 > 0$  such that:*

$$\mathbb{P} \left( \sup_{a \in \mathcal{A}} \left| \frac{\partial f}{\partial a^{(j)}} \right| > l \right) \leq C_2 \exp \left( -\frac{l^2}{C_3} \right), \text{ for } j \in \{1, \dots, d\} \text{ and } l > 0 \quad (8)$$

where  $a^{(j)}$  denotes the  $j$ -th element of  $a$ .

Whilst the high probability bound on the derivatives of the sample paths is a common assumption in the literature ([11, 31, 32, 14]), we additionally require that both  $\mu$  and  $k$  are Lipschitz. By [33, Thm. 5], the high probability bound holds if  $\mu$  is continuously differentiable and  $k$  is 4 times differentiable, which would also imply the Lipschitzness of  $\mu$  and  $k$ . As discussed in [11], this holds for the Matérn kernel if  $\nu \geq 2$  by a result of [34] and holds trivially for the squared exponential kernel. Thus, Lipschitzness of the kernel is not restrictive. Similarly, any continuously differentiable  $\mu$  is also Lipschitz.

Following [11], proofs for the compact case tend to use a discretization  $\mathcal{D}_t \subset \mathcal{A}$  where each dimension is divided into  $\tau_t$  points such that  $|\mathcal{D}_t| = \tau_t^d$ . Due to the varying arm availability, we require the following finer discretization (as compared to [14]):

**Assumption 2** (Discretization size). *Let  $\tau_t$  denote the number of discretization points per dimension and assume that*

$$\begin{cases} \tau_t \geq 2t^2 K L d C_1 (1 + t K \varsigma^{-1}), \\ \tau_t / \beta_t \geq 8t^4 K^2 L d C_1, \\ \tau_t^2 / \beta_t \geq 8t^5 K^3 L^2 d^2 C_1^2 \varsigma^{-2}, \\ \tau_t \geq t^2 K d C_1 C_3 \left( \sqrt{\log(C_2 d)} + \frac{\sqrt{\pi}}{2} \right) \end{cases} \quad (9)$$

where the constants  $C_1, C_2, C_3$  and  $L$  are given by Assumption 1 whilst the constants  $d, K$  and  $\varsigma$  are defined by the bandit problem (Section 2.1).

The final inequality in Assumption 2 is equivalent to the discretization size used by [14] with an extra factor of  $K$  to account for the combinatorial setting. Let  $[a]_{\mathcal{D}_t}$  denote the nearest point in  $\mathcal{D}_t$  for  $a \in \mathcal{A}$  and similarly let  $[\mathbf{a}]_{\mathcal{D}_t} = \{[a]_{\mathcal{D}_t} | a \in \mathbf{a}\}$  for  $\mathbf{a} \subset \mathcal{A}$ . Then, the first three inequalities in Assumption 2 allows us to bound the discretization error of the posterior mean and standard deviation as expressed by the following lemmas:

**Lemma 1.** *If Assumption 1 holds and  $\tau_t \geq 2t^2 K L d C_1 (1 + t K \varsigma^{-1})$ , then for any sequence of super arms  $\mathbf{a}_t \in \mathcal{S}_t$   $t \geq 1$ , the posterior mean  $\mu_{t-1}(\mathbf{a})$  satisfies*

$$\sum_{t \in [T]} \mathbb{E} [\mu_{t-1}([\mathbf{a}_t]_{\mathcal{D}_t}) - \mu_{t-1}(\mathbf{a}_t)] \leq \frac{\pi^2}{12}. \quad (10)$$

**Lemma 2.** *If Assumption 1 holds and  $\tau_t$  satisfies*

$$\tau_t / \beta_t \geq 8t^4 K^2 L d C_1 \text{ and } \tau_t^2 / \beta_t \geq 8t^5 K^3 L^2 d^2 C_1^2 \varsigma^{-2} \quad (11)$$

then, for any sequence of super arms  $\mathbf{a}_t \in \mathcal{S}_t$   $t \geq 1$ , the posterior standard deviation  $\sigma_{t-1}(\mathbf{a})$  satisfies

$$\sum_{t \in [T]} \mathbb{E} \left[ \sqrt{\beta_t} (\sigma_{t-1}([\mathbf{a}_t]_{\mathcal{D}_t}) - \sigma_{t-1}(\mathbf{a}_t)) \right] \leq \frac{\pi^2}{12}. \quad (12)$$

A key step to establish the regret bound of GP-UCB in [14] is to use the fact (for that setting) that  $\mathbf{a}_t$  optimizes the upper confidence bound  $U_t(\mathbf{a})$  and thus  $U_t([\mathbf{a}_t^*]_{\mathcal{D}_t}) - U_t(\mathbf{a}_t) \leq 0$ . Since we consider a setting with varying arm availability,  $[\mathbf{a}_t^*]_{\mathcal{D}_t}$  is not necessarily a feasible super arm, which necessitates Lemmas 1 and 2. Then, we present our regret bound for GP-UCB in the infinite setting:

**Theorem 3** (Infinite GP-UCB). *If Assumption 1 holds, then the Bayesian regret of GP-UCB with  $\beta_t = 2 \log(\tau_t^d t^2 / \sqrt{2\pi})$  is bounded by:*

$$\text{BayesRegret}(T) \leq \frac{\pi^2}{2} + \sqrt{C_4 T K \beta_T \gamma_{TK}} \quad (13)$$

where  $\tau_t$  satisfies Assumption 2 and  $C_4 = 2 / \log(1 + \varsigma^{-2})$ .

The regret bound for Bayes-GP-UCB requires us to work around the non-elementary function  $\text{erf}^{-1}(u)$ . Using [35, Thm. 2], it is possible to establish that  $\text{erf}^{-1}(u) \geq \sqrt{-\omega^{-1} \log((1-u)/\vartheta)}$  for  $\omega > 1$  and  $0 < \vartheta \leq \sqrt{2e/\pi} \sqrt{\omega-1}/\omega$ , see Lemma 17. The bound is tighter for larger values of the parameter  $\vartheta$  [35], thus we set  $\vartheta$  to its maximum value whilst  $\omega$  is kept as a tunable parameter. We establish regret bounds where the quantile parameter  $\eta_t$  is of order  $\mathcal{O}(t^{-\xi})$  for any  $\xi > 0$ :

**Theorem 4** (Infinite Bayes-GP-UCB). *If Assumption 1 holds, then the Bayesian regret of Bayes-GP-UCB with  $\beta_t = 2 \left(\text{erf}^{-1}(1 - 2\eta_t)\right)^2$  for  $\eta_t = (2\pi)^{\omega/2} / (2\tau_t^{d\omega} t^\gamma)$ ,  $\omega > 1$  is bounded by:*

$$\text{BayesRegret}(T) \leq \frac{\pi^2}{3} + \sqrt{C_4 T K \beta_T \gamma_{TK}} + \left( \frac{\sqrt{\pi\omega}}{\sqrt{2e(\omega-1)}} \right)^{1/\omega} \begin{cases} \frac{\omega}{\omega-\xi} T^{1-\frac{\xi}{\omega}} & \text{if } \xi/\omega < 1, \\ \frac{\xi}{\xi-\omega} & \text{if } \xi/\omega > 1. \end{cases} \quad (14)$$

where  $\tau_t$  satisfies Assumption 2 and  $C_4 = 2/\log(1 + \zeta^{-2})$ .

Establishing regret bounds for GP-TS relies on the fact that the optimal arm and the selected arm have the same distribution given  $H_t$ , that is  $\mathbf{a}_t^* | H_t \stackrel{d}{=} \mathbf{a}_t | H_t$ .

**Theorem 5** (Infinite GP-TS). *If Assumption 1 holds, then the Bayesian regret of GP-TS is bounded by:*

$$\text{BayesRegret}(T) \leq \frac{2\pi^2}{3} + 2\sqrt{C_4 T K \beta_T \gamma_{TK}} \quad (15)$$

where  $\beta_t = 2 \log(\tau_t^{d_t} t^2 / \sqrt{2\pi})$  with  $\tau_t$  satisfying Assumption 2 and  $C_4 = 2/\log(1 + \zeta^{-2})$ .

Since the selected arm given the history,  $\mathbf{a}_t | H_t$ , is random for GP-TS, the regret must be decomposed into more terms compared to GP-UCB, which increases the constants in the bound.

## 4 Case Study: Online Energy-Efficient Navigation

An important and relevant application of the combinatorial and contextual bandit problem that we analyze in Section 3 is the problem of online energy-efficient navigation for electric vehicles. Previous work by Åkerblom et al. [28] introduced a framework based on Bayesian inference to address the online navigation problem when no contextual information is available. In this case study, we use Gaussian processes to extend the framework of [28] to the contextual setting.

### 4.1 Formulation of online energy-efficient navigation

In this section, we frame the problem of online energy-efficient navigation as a bandit problem using the problem formulation introduced in Section 2.1.

Consider a directed graph  $\mathcal{G}(\mathcal{V}, \mathcal{E})$  where the vertices  $\mathcal{V}$  denote intersections of road segments and the edges  $e = (u_1, u_2) \in \mathcal{E}$  denote the road segment from intersection  $u_1$  to intersection  $u_2$ . Additionally, let  $\mathcal{L}(\mathcal{G}) = \mathcal{G}(\mathcal{E}, \mathcal{C}_t)$  denote the directed line graph of  $\mathcal{G}$  where the set of connections  $\mathcal{C}_t$  between directed edges determine which turns are legal in the road network at time  $t$ :  $\mathcal{C}_t \subseteq \{(e_1, e_2) | e_1 = (u, v) \in \mathcal{E}, e_2 \in (v, w) \in \mathcal{E}\}$ .

Assume that we are given a start vertex  $u_1 \in \mathcal{V}$  and a goal vertex  $u_n \in \mathcal{V}$ . Let  $\mathcal{P}_t$  denote the set of legal and simple paths from  $u_1$  to  $u_n$  at time  $t$ . A path  $\mathbf{p} = \langle u_1, u_2, \dots, u_n \rangle$  is legal if all the connections are legal, and  $\mathbf{p}$  is simple if every vertex is visited at most once.

At each time step  $t$ , we observe the set of available paths  $\mathcal{P}_t$  and a context vector  $x_{t,e} \in \mathbb{R}^d$  for each edge  $e \in \mathcal{E}$ . The context  $x_{t,e}$  can include static features, such as the length of the road segment, and time-varying features, such as the congestion level. Based on the available connections and the context vector, we select a path  $\mathbf{p}_t \in \mathcal{P}_t$  and observe the energy consumption associated with each edge in the path (negated reward):  $R_t = \sum_{e \in \mathbf{p}_t} r_{t,e}$ . The goal of energy-efficient navigation is to minimize the total energy consumed over a horizon  $T$ .

Note that base arm set  $\mathcal{A}_t$  corresponds to all edge-context tuples  $(e, x_{t,e})$  and that the base arm space is defined as  $\mathcal{A} = \mathcal{E} \times \mathcal{X}$  where  $\mathcal{X} \subseteq [0, r]^d$  is a compact and convex set for some  $r > 0$ . The super arm set  $\mathcal{S}_t$  corresponds to sequences of edge-context tuples that form paths in  $\mathcal{P}_t$ .

### 4.2 Energy model and shortest path

The energy consumption of driving along a road segment is stochastic in practice. As in [28], we model it using a Bayesian approach in order to incorporate both prior knowledge and observations from the environment. The prior

---

**Algorithm 2** Gaussian parameter update of the energy model

---

```
1: procedure UPDATEPARAMETERS( $\mathbf{a}_t, \mathbf{r}_t, \boldsymbol{\theta}_{t-1} = (\boldsymbol{\mu}_{t-1}, \boldsymbol{\sigma}_{t-1}, \boldsymbol{\varsigma}_{t-1})$ )
2:   for each edge  $e \in \mathbf{a}_t$  do
3:      $\sigma_{t,e}^2 \leftarrow (\sigma_{t-1,e}^{-2} + \varsigma_{t-1,e}^{-2})^{-1}$ 
4:      $\mu_{t,e} \leftarrow \sigma_{t,e}^2 (\mu_{t-1,e} \sigma_{t-1,e}^{-2} + r_{t,e} \varsigma_{t-1,e}^{-2})$ 
5:    $\boldsymbol{\varsigma}_t \leftarrow \boldsymbol{\varsigma}_{t-1}$ 
6:   return  $(\boldsymbol{\mu}_t, \boldsymbol{\sigma}_t, \boldsymbol{\varsigma}_t)$ 
```

---

knowledge consists of a simplified deterministic model for the energy consumption. The deterministic model assumes that the vehicle drives along an edge  $e \in \mathcal{E}$ , with length  $\ell_e$  and inclination  $\alpha_e$ , at constant speed  $v_e$ :

$$E_e^{\text{det}} := \frac{mgl_e \sin(\alpha_e) + mgC_r \ell_e \cos(\alpha_e) + 0.5C_d A \rho \ell_e v_e^2}{3600\eta}. \quad (16)$$

The deterministic energy consumption  $E_e^{\text{det}}$  in Eq. (16) is given in Watt-hours and depends on the following vehicle-specific parameters: mass  $m$ , rolling resistance  $C_r$ , front surface area  $A$ , air drag coefficient  $C_d$  and powertrain efficiency  $\eta$ . The gravitational acceleration  $g$  and air density  $\rho$  also determine  $E_e^{\text{det}}$ .

A benefit of electric vehicles is their ability to recuperate energy by using *regenerative braking*. With regenerative braking, the energy consumption of an electric vehicle can be negative along individual road segments, which presents challenges when we wish to find the most energy-efficient path. The most common shortest path algorithm, Dijkstra’s algorithm [36], does not permit negative edge weights. Whilst alternative shortest path algorithms, such as Bellman-Ford [37, 38, 39], allow negative edge weights, they are significantly slower and do not return a path if the graph has a reachable negative cycle. In fact, for graphs with negative cycles, the problem of finding the shortest simple path is NP-hard [40]. To avoid the complexity associated with negative weights, we use the rectified normal distribution to get non-negative energy consumption estimates as input for Dijkstra’s algorithm, see Section 4.5.

### 4.3 Bayesian inference for energy-efficient navigation

In this section, we introduce the Bayesian inference method used in [28] to learn the distribution of the energy consumption in each road segment. The key assumption is that the energy consumption,  $E_e \in \mathbb{R}$ , of an electric vehicle driving along the road segment  $e \in \mathcal{E}$  is stochastic and follows a Gaussian distribution with unknown mean  $\mu_e^*$  and known variance  $(\varsigma_e^*)^2$ . Additionally, it is assumed that the energy consumption along different edges is independent,  $E_e \perp E_{e'} \forall e' \in \mathcal{E} \setminus \{e\}$ .

The likelihood function of the Bayesian inference model is given by

$$p(E_e | \mu_e^*, (\varsigma_e^*)^2) := \mathcal{N}(E_e | \mu_e^*, (\varsigma_e^*)^2). \quad (17)$$

Similarly, we use a Gaussian conjugate prior for the mean parameter  $\mu_e^*$ :

$$p(\mu_e^* | \mu_{0,e}, \sigma_{0,e}^2) = \mathcal{N}(\mu_e^* | \mu_{0,e}, \sigma_{0,e}^2), \quad (18)$$

where  $\mu_{0,e}$  and  $\sigma_{0,e}^2$  are the prior mean and variance respectively. Section 5.2.1 describes the initialization of the prior parameters. The conjugate prior provides simple update equations for the posterior parameters  $\mu_{t,e}$  and  $\sigma_{t,e}^2$ , see Algorithm 2.

### 4.4 GP regression for energy-efficient navigation

Since the Bayesian inference method introduced in [28] (see Section 4.3) assumes that the energy consumption of each edge is independently distributed, it cannot utilize correlations that may exist naturally to learn more efficiently. In this section, we describe our Gaussian process method for online learning of energy-efficient navigation. To our knowledge, this is the first combinatorial Gaussian process bandit solution for energy-efficient navigation.

#### 4.4.1 Kernel design

To capture the energy consumption’s dependency on the structure of the graph and the provided context, we utilize kernel compositions to embed both these dependencies into the model. To embed the structure of the graph, we extend the graph Matérn GP from [41] to the edges of a directed graph by considering the incidence graph Laplacian of the line graph  $\mathcal{L}(\mathcal{G})$ . The original graph Matérn GP defines a GP on the vertices of a weighted and undirected graph.

---

**Algorithm 3** SVGP Optimization Procedure
 

---

- 1: **procedure** UPDATEPARAMETERS( $\mathbf{a}_t, \mathbf{r}_t, \boldsymbol{\theta}_{t-1}$ )
  - 2:   Set inducing points  $\mathbf{Z}_t$  to top  $M$  most visited edges.
  - 3:   **for**  $i \in \{1, \dots, \#\text{gradient steps}\}$  **do**
  - 4:      $\tilde{\mathbf{a}}, \tilde{\mathbf{r}} \leftarrow$  Subsample batch of size  $B$  from all observations.
  - 5:     Compute batch ELBO.
  - 6:     Optimize variational parameters with natural gradient descent.
  - 7:     Optimize kernel and likelihood parameters with Adam.
  - 8:   Compute  $\boldsymbol{\mu}_t, \boldsymbol{\sigma}_t, \boldsymbol{\varsigma}_t$  using the optimized GP parameters.
  - 9:   **Return**  $\boldsymbol{\mu}_t, \boldsymbol{\sigma}_t, \boldsymbol{\varsigma}_t$  and optimized GP parameters.
- 

Let  $\mathbf{W}_{\mathcal{L}} \in \mathbb{R}^{|\mathcal{E}| \times |\mathcal{C}|}$  denote the weight matrix of  $\mathcal{L}(\mathcal{G}) = (\mathcal{E}, \mathcal{C})$ . The weight  $W_{\mathcal{L}, e_1, e_2}$  is set to  $\bar{\ell}/\ell_{e_1}$  where  $\bar{\ell}$  is the average length of all edges and  $\ell_{e_1}$  is the length of edge  $e_1$ . We replace the ordinary graph Laplacian used in [41] with the incidence Laplacian:

$$\boldsymbol{\Delta}_I = \mathbf{B}\mathbf{B}^\top, \quad (19)$$

where the incidence matrix  $\mathbf{B} \in \mathbb{R}^{|\mathcal{E}| \times |\mathcal{C}|}$  has entries

$$B_{e,c} = \begin{cases} -W_{\mathcal{L}, e_1, e_2} & \text{if } e = e_1, \\ W_{\mathcal{L}, e_1, e_2} & \text{if } e = e_2, \\ 0 & \text{otherwise} \end{cases} \quad \forall e \in \mathcal{E}, c = (e_1, e_2) \in \mathcal{C}. \quad (20)$$

Let  $\boldsymbol{\Delta}_I = \mathbf{U}_I \boldsymbol{\Lambda}_I \mathbf{U}_I^\top$  denote the eigendecomposition of  $\boldsymbol{\Delta}_I$ , then the graph Matérn GP of the edges is given by

$$\mathbf{f} \sim \mathcal{N} \left( 0, \mathbf{U}_I \left( \frac{2\nu_G}{\kappa_G^2} \mathbf{I} + \boldsymbol{\Lambda}_I \right)^{-\nu} \mathbf{U}_I^\top \right). \quad (21)$$

Let  $k_G : \mathcal{E} \times \mathcal{E} \rightarrow \mathbb{R}$  denote the corresponding graph kernel with an additional outputscale parameter  $\sigma_G$ . For large graphs, we approximate  $k_G$  by using the 500 smallest eigenpairs of  $\boldsymbol{\Delta}_I$ .

Next, let  $k_f : \mathbb{R}^d \times \mathbb{R}^d \rightarrow \mathbb{R}$  denote a feature kernel which measures the similarity between the contexts of the edges. In this work, we use an ordinary Matérn kernel with fixed  $\nu = 5/2$  but tunable outputscale  $\sigma_f$  and lengthscales  $\boldsymbol{\ell}_f \in \mathbb{R}_+^d$  for each dimension:

$$k_f(x_e, x_{e'}) := \sigma_f \frac{2^{1-\nu}}{\Gamma(\nu)} \left( \sqrt{2\nu} D \right)^\nu K_\nu \left( \sqrt{2\nu} D \right), \quad (22)$$

where  $x_e$  denotes the feature vector of edge  $e$  and the feature distance  $D$  between edge  $e$  and  $e'$  is given by

$$D = \sqrt{(x_e - x_{e'})^\top \text{diag}(\boldsymbol{\ell}_f)^{-2} (x_e - x_{e'})}. \quad (23)$$

In addition to the two basic kernels,  $k_G$  and  $k_f$ , we define the following shorthand notation for composing the two kernels:  $k_{G+f} = k_G + k_f$ ,  $k_{G \cdot f} = k_G \cdot k_f$  and  $k_{G \cdot f + f} = k_G \cdot k_f + k'_f$ . Note that for  $k_{G \cdot f + f}$ , the two feature kernels do not share parameters which allows the kernel to be more expressive.

#### 4.4.2 Sparse Variational GPs

The cubic cost of exact GPs prohibit their application to large datasets. Sparse Variational Gaussian processes (SVGPs) [42, 43] approximate the posterior distribution using a set of inducing points  $\mathbf{Z}_t = \{z_1, \dots, z_M\}$  where  $z_i \in \mathcal{A}$  and  $M$  is significantly smaller than the number of datapoints. By defining a prior distribution  $q(\mathbf{u}_t) = \mathcal{N}(\mathbf{m}_t, \mathbf{S}_t)$  for the inducing variables  $\mathbf{u}_t$ , an approximate GP posterior can be obtained such that the complexity to perform  $N$  predictions is  $\mathcal{O}(M^2 N)$ , i.e. linear w.r.t.  $N$ . The kernel and likelihood parameters can be optimized jointly with  $(\mathbf{m}_t, \mathbf{S}_t)$  by minimizing the evidence lower bound (ELBO) using stochastic gradient descent at a cost of  $\mathcal{O}(BM^2 + M^3)$  with batch size  $B$ . A more detailed description of SVGP can be found in [44].

Since the inducing points  $z_i$  lie in a mixed discrete and continuous space ( $\mathcal{A} = \mathcal{E} \times \mathcal{X}$  for  $\mathcal{X} \subset [0, r]^d$ ), we heuristically set  $z_i$  equal to the edge-context tuple of the  $i$ -th most visited edge at the start of the SVGP optimization. Then, the continuous dimensions of  $z_i$  is optimized together with  $(\mathbf{m}_t, \mathbf{S}_t)$  using natural gradient ascent [45]. The kernel and likelihood parameters are optimized using Adam [46]. The procedure is described in Algorithm 3.



---

**Algorithm 4** Thompson sampling

---

- 1: **procedure** GETBASEARMINDICES( $t, \mathcal{A}_t, \theta_{t-1} = (\mu_{t-1}, \sigma_{t-1}, \varsigma_{t-1})$ )
  - 2:   **for** each edge  $e \in \mathcal{A}_t$  **do**
  - 3:      $\tilde{\mu}_e \leftarrow$  Sample from posterior  $\mathcal{N}(\mu_{t-1,e}, \sigma_{t-1,e}^2)$
  - 4:      $U_{t,e} \leftarrow \mathbb{E}[z_e]$  where  $z_e \sim \mathcal{N}^R(\tilde{\mu}_e, \varsigma_{t-1,e}^2)$
  - 5:   **return**  $U_t$
- 

---

**Algorithm 5** Bayesian Upper Confidence Bounds

---

- 1: **procedure** GETBASEARMINDICES( $t, \mathcal{A}_t, \theta_{t-1} = (\mu_{t-1}, \sigma_{t-1}, \varsigma_{t-1})$ )
  - 2:   **for** each edge  $e \in \mathcal{A}_t$  **do**
  - 3:      $\tilde{\mu}_e \leftarrow Q(\frac{1}{t}, \mathcal{N}(\mu_{t-1,e}, \sigma_{t-1,e}^2))$
  - 4:      $U_{t,e} \leftarrow \mathbb{E}[z_e]$  where  $z_e \sim \mathcal{N}^R(\tilde{\mu}_e, \varsigma_{t-1,e}^2)$
  - 5:   **return**  $U_t$
- 

## 4.5 TS and Bayes-UCB with rectified Gaussians

As discussed in Section 4.2, feasibly computing the shortest path requires non-negative edge weights  $U_{t,e}$ . Thompson sampling and Bayes-UCB output real posterior estimates  $\tilde{\mu}_e$  either by sampling or by producing optimistic bounds from the posterior  $\mathcal{N}(\mu_{t-1,e}, \sigma_{t-1,e}^2)$ . To ensure non-negative weights, the edge weight  $U_{t,e}$  is set to  $\mathbb{E}[z_e]$  where  $z_e$  is distributed as the rectified Gaussian  $\mathcal{N}^R(\tilde{\mu}_e, \varsigma_{t-1,e}^2)$ . A random variable  $Y = \max(0, X)$  is said to have a rectified Gaussian distribution  $\mathcal{N}^R(\mu, \sigma^2)$  if the variable  $X \sim \mathcal{N}(\mu, \sigma^2)$  and the mean of  $Y$  is given by  $\mathbb{E}[Y] = \mu(1 - \Phi(-\mu/\sigma)) + \sigma\phi(-\mu/\sigma)$  where  $\Phi$  and  $\phi$  is the CDF and PDF of the standard Gaussian distribution [47, 48, 49]. See Algorithms 4 and 5 to understand how the methods integrate with the framework in Algorithm 1.

The notation  $\mu_{t-1,e}, \sigma_{t-1,e}^2$  refers to the posterior mean and variance of the expected energy consumption for edge  $e$  whilst  $\varsigma_{t-1,e}^2$  refers to the variance of the noise. Algorithms 4 and 5 work for both the Bayesian inference and the GP method but it is worth noting that  $\mu_{t-1,e}$  and  $\sigma_{t-1,e}^2$  depend on the observed context  $x_{t,e}$  for the GP method, which has been omitted to simplify notation. Since the number of edges  $|\mathcal{E}|$  may be very large, each edge is sampled independently in TS, as in [20]. Additionally, Bayes-UCB uses the lower  $1/t$  quantile similar to [28] since we wish to minimize energy consumption.

The main focus of this study is to evaluate the impact of the contextual GP method. Due to the similarity between GP-UCB and Bayes-GP-UCB, we restrict ourselves to consider Bayes-GP-UCB and GP-TS - similar to [28].

## 5 Experiments

In this section, we experimentally study the online energy-efficient navigation problem for electric vehicles. We are primarily interested in understanding the efficiency and applicability of the GP regression model introduced in Section 4.4. We, thereby, investigate the impact of various design choices (GP vs. non-GP formulation, bandit algorithm, kernel function, prior, inducing points and noise model) in a principled way. First, we introduce the road networks, the experimental setup and our evaluation metrics. Finally, we present and discuss the experimental results in different settings.

### 5.1 Road networks

We conduct our experiments on two types of road networks: i) synthetic networks with known ground-truth, and ii) real-world road networks for Luxembourg and Monaco.

#### 5.1.1 Synthetic network

The purpose of the synthetic network is to be simple but non-trivial, to evaluate the GP model against a known ground-truth. The network is visualized in Fig. 1. To construct the graph of the network, the vertices are initially given  $x$  and  $y$  coordinates in a regular grid of size  $10 \times 10$  with side-length of 1 m, thus  $|\mathcal{V}| = 100$ . Adjacent vertices are connected with bidirectional edges. The coordinates of each vertex are perturbed with Gaussian noise from  $\mathcal{N}(0, 0.3^2)$  to make the network irregular and more difficult to traverse. Elevation is added to each vertex by sampling  $z$ -coordinates

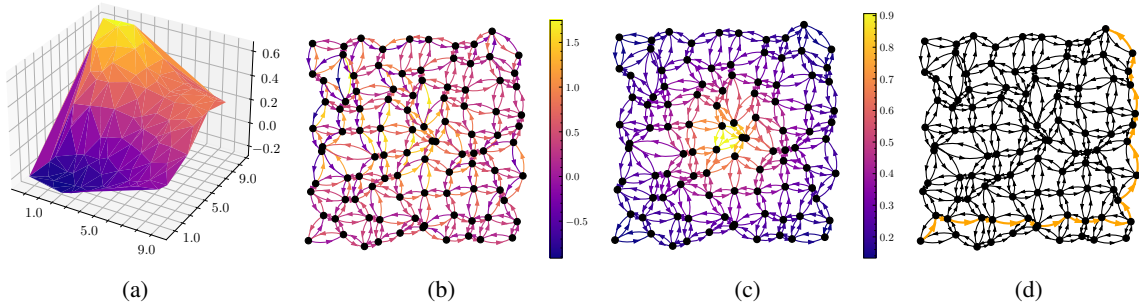


Figure 1: Synthetic road network with a) elevation, b) expected energy consumption, c) cluster energy consumption and d) most energy-efficient path from the bottom-left to the top-right.

Table 1: The number of vertices, edges and connections in the real-world road networks. The subcomponent is the largest strongly connected component.

City	Complete			Subcomponent		
	$ \mathcal{V} $	$ \mathcal{E} $	$ \mathcal{C} $	$ \mathcal{V} $	$ \mathcal{E} $	$ \mathcal{C} $
Luxembourg	2247	5779	11 286	1940	5169	10 133
Monaco	1766	3613	5838	1659	3474	5660

from a GP in  $\mathbb{R}^2$ , using the RBF-kernel with lengthscale 2 in both dimensions and the output scaled by the factor of 0.1 (see Fig. 1a for a visualization). Using the  $x$ -,  $y$ - and  $z$ -coordinates, we compute the length and incline of each edge. The speed of each edge is set to 50 km/h plus Gaussian noise from  $\mathcal{N}(0, 2^2)$ .

Using the vehicle and environmental parameters in Table 2, the energy consumption of the deterministic model  $E_e^{\text{det}}$  is computed as described by Eq. (16). To model pseudo-congestion in the network, an additional term is added to the energy consumption that we refer to as the cluster energy consumption. The cluster energy consumption is determined by the Euclidean distance between the edge and the center of the graph, i.e.,

$$E_{e,c} = \exp\left(-\sqrt{(\tilde{x}_e - \tilde{x}_g)^2 + (\tilde{y}_e - \tilde{y}_g)^2} / 3\right), \quad (24)$$

where the edge coordinates  $\tilde{x}_e$  and  $\tilde{y}_e$  for edge  $e = (u, v)$  correspond to the edge midsection. The graph center coordinates  $(\tilde{x}_g, \tilde{y}_g)$  are set as the average of all vertex coordinates. See Fig. 1c for a visualization of the cluster energy consumption. The true expected energy consumption is then  $\mu_e^* = E_e^{\text{det}} + E_{e,c}$  and the true variance of the energy consumption is set to  $(\varsigma_e^*)^2 = (0.25 \cdot \mu_e^*)^2$ . The most energy-efficient path from the start vertex to the end vertex is visualized in Fig. 1d.

### 5.1.2 Real-world road networks

To simulate real-world road networks, the simulator SUMO [50] (v.1.16.0) is combined with traffic scenarios and networks of two European cities: Monaco [51] and Luxembourg [52]. Whilst the Monaco network includes elevation data, we add elevation data from [53] to the Luxembourg network using QGIS [54] and the *netconvert* tool from SUMO. Adding the elevation data invalidates the position of certain bus stops and traffic detectors in the Luxembourg scenario. We recompute valid positions by considering the prior relative position of the object along the edge and rescale it based on the new length.

To conveniently be able to select edges to travel between, we restrict the road networks to the largest strongly connected component of the line graph  $\mathcal{L}(G)$ . Table 1 shows the number of vertices, edges, and connections for the complete and restricted networks. The restriction has a minor impact on Luxembourg, where many smaller residential roads lack U-turns, but this should not affect the navigational difficulty.

Due to unforeseen crashes in SUMO, we could not use the same simulation setup for Monaco and Luxembourg. For Luxembourg, the network was simulated for 24 hours, and the state of the simulation was saved every 100 seconds. For each timestep  $t$  in the bandit problem, the simulation was started using a randomly selected state. For Monaco, the simulation was started with a network without any active vehicles at a randomly selected time between 04:00 and 14:00

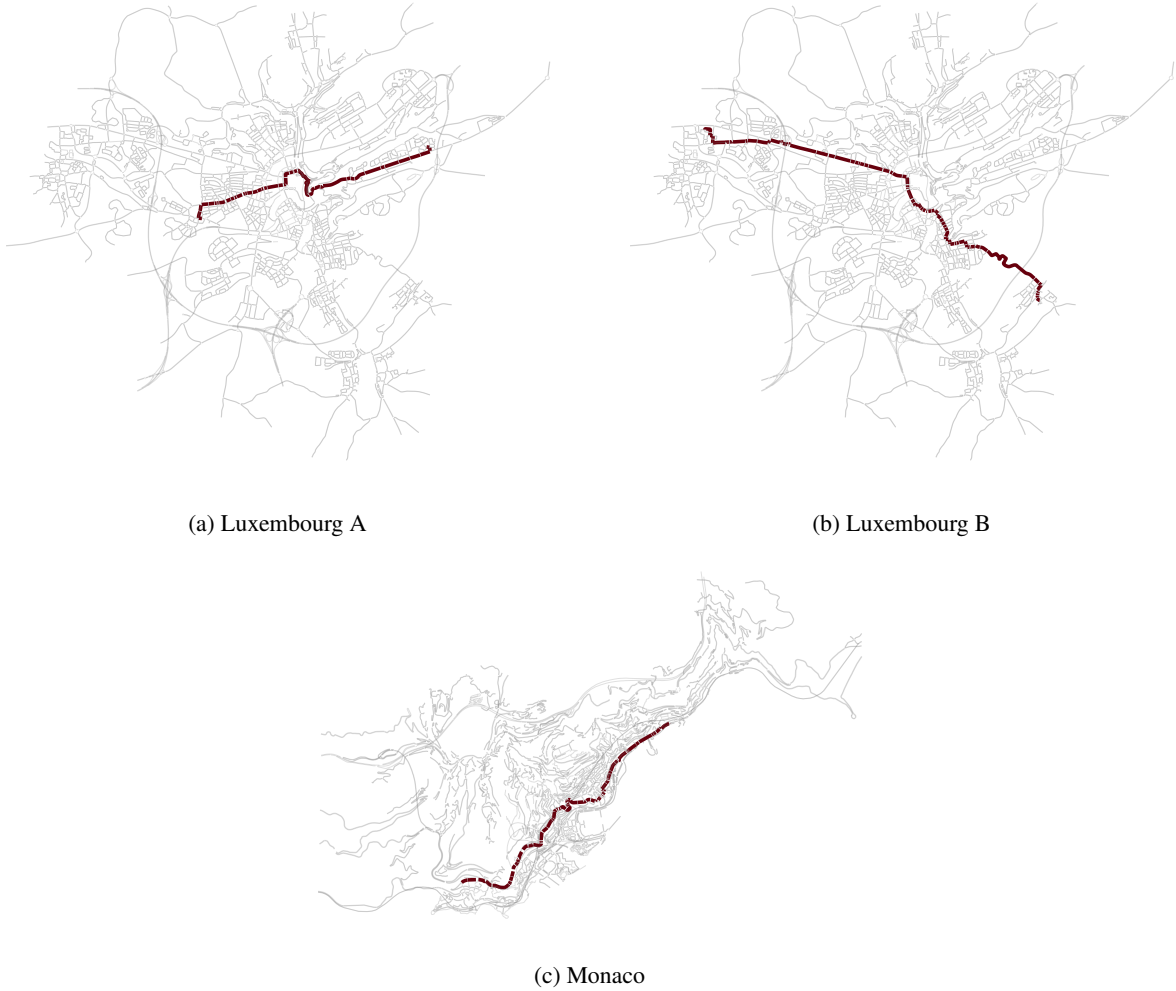


Figure 2: The road networks of a-b) Luxembourg and c) Monaco with evaluation routes highlighted.

at each time step  $t$ . Although the Monaco simulation initializes vehicles over time, the traffic will be underestimated in the busiest hours since the congestion is unable to build up.

In Fig. 2, the two road networks are visualized along with evaluation routes. The evaluation routes involve multiple regions of the respective networks, thus allowing for many alternative paths. Two evaluation routes are used for Luxembourg since it has a larger road network and more realistic traffic.

## 5.2 Experimental setup

Here, we describe the choice of priors used, the default parameter values of the methods and vehicles, as well as the evaluation metrics.

### 5.2.1 Informative priors

We use three different priors for both Bayesian inference and the GP model that determine  $\mu_0$ ,  $\sigma_0$  and  $\varsigma_0$ . The priors have different levels of informativeness.

The first prior provides the most information and is referred to as the *full* prior. For the full prior, we let  $\mu_{e,0} = E_e^{\text{det}}$ ,  $\sigma_{e,0}^2 = (0.25E_e^{\text{det}})^2$  and  $\varsigma_{e,0}^2 = (0.1E_e^{\text{det}})^2 \forall e \in \mathcal{E}$ . The full prior provides a good but simple estimation of the expected energy consumption, where both the prior and noise standard deviations are scaled proportionally to the prior mean.

Table 2: Vehicle and environmental parameters for the energy model.

Variable	Value	Unit
Mass $m$	1830	kg
Rolling resistance coefficient $C_r$	0.01	
Front surface area $A$	2.6	m <sup>2</sup>
Air drag coefficient $C_d$	0.35	
Power train efficiency $\eta^+$	0.98	
Recuperation efficiency $\eta^-$	0.96	
Gravitational acceleration $g$	9.82	m/s <sup>2</sup>
Air density $\rho$	1.2	kg/m <sup>3</sup>

In the second prior, the values are initialized *uniformly*, which provides less information to the model overall but still gives the model the correct scale. Let  $\overline{E^{\text{det}}} = \frac{1}{|\mathcal{E}|} \sum_{e \in \mathcal{E}} E_e^{\text{det}}$  and  $\sigma^{\text{det}} = \sqrt{\frac{1}{|\mathcal{E}|} \sum_{e \in \mathcal{E}} (E_e^{\text{det}} - \overline{E^{\text{det}}})^2}$  denote the mean and standard deviation of the deterministic energy consumption. Then, the uniform prior assigns the following,  $\mu_{e,0} = \overline{E^{\text{det}}}$ ,  $\sigma_{e,0}^2 = (0.25\sigma^{\text{det}})^2$  and  $\varsigma_{e,0}^2 = (0.1\sigma^{\text{det}})^2 \forall e \in \mathcal{E}$ .

Finally, in the third prior we assign an *optimistic* mean and uniform variance:  $\mu_{e,0} = 0$ ,  $\sigma_{e,0}^2 = (0.25\sigma^{\text{det}})^2$  and  $\varsigma_{e,0}^2 = (0.1\sigma^{\text{det}})^2 \forall e \in \mathcal{E}$ . The optimistic prior provides a misleading prior for most edges where the expected energy consumption is positive.

The GP model does not support initial parameters equivalent to  $\sigma_0$  and  $\varsigma_0$  for each edge. Thus for the full prior, the kernel outputscale parameters  $\sigma_f^2$  and  $\sigma_G^2$  are set to  $\sigma_0^\top \sigma_0 / |\mathcal{E}|$ , and the likelihood variance  $\varsigma^2$  is set to  $\varsigma_0^\top \varsigma_0 / |\mathcal{E}|$ . However, since the parameters are later optimized in Algorithm 3, this should not hinder the GP model.

## 5.2.2 Parameters

In this section, we specify the default parameter values for the electric vehicle model and the GP model. If nothing else is specified in specific experiments, then the parameter values given in this section are used. We use the default parameters for electric vehicles provided by SUMO [50], see Table 2.

We standardize the edge features of each network and set the initial ARD lengthscale to 1 for all features in the GP models. The graph kernel is initialized with parameters  $\nu_G = 2$ ,  $\kappa_G = 1$  and  $\sigma_G$  set according to the prior. The natural gradient descent learning rate is set to 0.1 whilst the Adam learning rate is set to 0.01. Both the GP and Bayesian inference models use Thompson sampling and the uniform prior. The GP model uses homoskedastic noise modeling as standard.

In the synthetic network, the GP models use a batch size  $B$  of 2500 and 1 gradient step per optimization procedure in Algorithm 3. The number of inducing points equals the number of edges.

In the simulated networks, the GP models use a batch size  $B$  of 8000 and 5 gradient steps per optimization procedure. The simulated scenarios are CPU-bottlenecked, thus the added optimization steps does not add significantly to the run time. The number of inducing points is set to 1000.

## 5.2.3 Evaluation metrics

For the synthetic road network, cumulative regret is used to measure the difference between the online learning models and the optimal route. The optimal expected reward  $\mathbf{r}^*$  and the expected reward  $\mathbb{E}[\mathbf{r}_t]$  are computed using the negation of the true rectified weights:

$$w_e^* \leftarrow \mathbb{E}[z_e] \text{ where } z_e \sim \mathcal{N}^R(\mu_e^*, (\varsigma_e^*)^2). \quad (25)$$

If the optimal path is given by  $\mathbf{p}^*$  and the path selected at step  $t$  is given by  $\mathbf{p}_t$ , then  $\mathbf{r}^* = \sum_{e \in \mathbf{p}^*} -w_e^*$  and  $\mathbb{E}[\mathbf{r}_t] = \sum_{e \in \mathbf{p}_t} -w_e^*$ . The cumulative regret is then given as

$$\text{CumulativeRegret}(T) = \sum_{t=1}^T (\mathbf{r}^* - \mathbb{E}[\mathbf{r}_t]). \quad (26)$$

Since the true parameters  $\mu_e^*$  and  $(\varsigma_e^*)^2$  are unknown in the real-world road networks, neither  $\mathbf{r}^*$  nor  $\mathbb{E}[\mathbf{r}_t]$  can be calculated. Therefore, we use the *random regret* metric for the simulated real-world networks. For a given set of

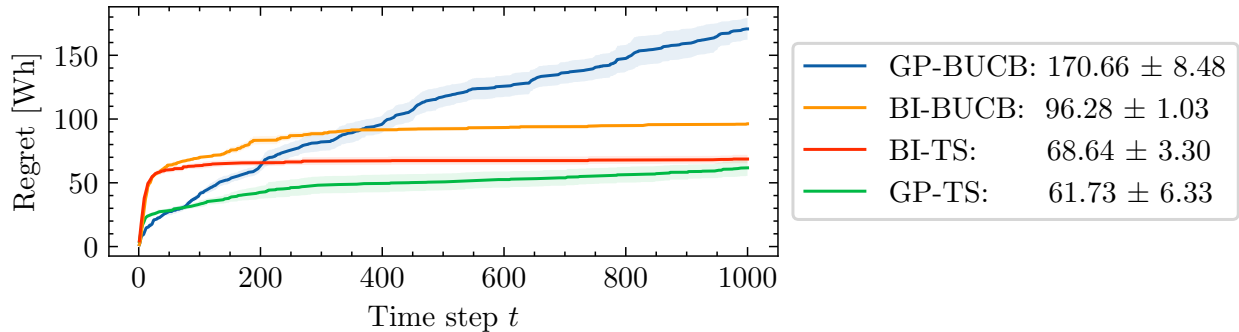


Figure 3: Cumulative regret on the synthetic network for different bandit algorithms. Average and standard error of the final cumulative regret to the right.

observations of the energy consumption along each route obtained in Algorithm 1,  $\{\mathbf{r}_t\}_{t=1}^T$ , the random regret is defined as

$$\text{RandomRegret}(T) = \sum_{t=1}^T (\hat{\mathbf{r}} - \mathbf{r}_t), \quad (27)$$

where  $\hat{\mathbf{r}}$  is the negation of the estimated cost of the most energy-efficient route. We compute the average energy consumption across the last 25 time steps for each run and then use the minimum as our estimate of the average lowest energy route  $\hat{\mathbf{r}}$ . Note that the estimates are computed separately for each comparison study and evaluation route.

In principle, if a model has identified a strictly better route, it should drive along this route in the final time steps. Inspecting the selection frequency of the observed lowest energy routes reveals that most routes are only driven once. By averaging across the 25 last time steps, we reduce the risk of underestimating the lowest energy route due to an outlier.

Note that random regret uses the observed energy consumption and thus the contribution of the energy recuperation is correctly accounted for. Additionally, since we subtract the same estimate from all runs in the same experiment, the difference in random regret equals the difference in total energy consumed.

To measure the models' ability to estimate the noise, we use the metric quantile coverage error (QCE). Given a  $q\%$ -confidence interval and a set of datapoints, the QCE measures the accuracy of the confidence interval. For example, if  $p\%$  of the datapoints lie in a  $q\%$ -confidence interval then the QCE is  $|p - q|\%$ . For a given confidence level  $q$  and QCE, the percentage of datapoints in the confidence interval is not necessarily unique and thus we use three confidence levels to understand if the model under- or overestimates the noise.

### 5.3 Results

In the following sections, we further describe the comparisons and present the experimental results.

#### 5.3.1 Investigation of bandit algorithms

To study the impact of the bandit algorithm on the GPs' performance and exploration, we compare Bayes-UCB (BUCB) and Thompson sampling (TS) on the synthetic network and the real-world networks of Luxembourg B and Monaco. As discussed in Section 2.2, UCB and Bayes-UCB differ only in their definition of the confidence parameter  $\beta_t$ , and therefore we consider only Bayes-UCB, similar to [28]. The two bandit algorithms are evaluated using the GP and the Bayesian inference (BI) models introduced in Sections 4.3 and 4.4, respectively.

For both the GP and BI models, the two bandit algorithms are run 10 times with a horizon of  $T = 1000$  on the synthetic network. For the real-world networks, we run each combination 5 times with  $T = 200$ .

In Fig. 3, the cumulative regret of BUCB and TS on the synthetic network is visualized for both the GP and Bayesian inference model. At the start, the GP models have lower regret than the equivalent Bayesian inference models. By the end, the GP-BUCB model does not find a stable route and the regret diverges from the rest. The cumulative regret for the Bayesian inference models is almost flat by the end, indicating that they identify the best route and almost always select it. The GP-TS model is initially successful in finding low-regret routes but is not as stable as BI-TS in the end.

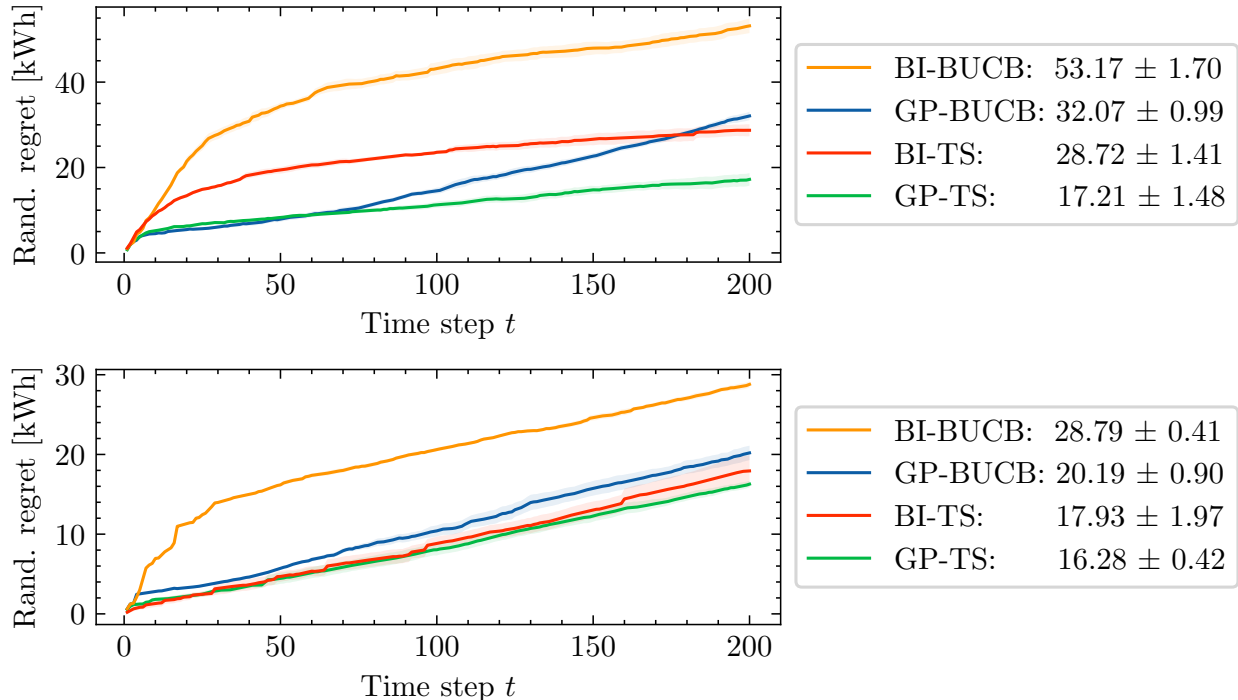


Figure 4: Random regret on Luxembourg B (top) and Monaco (bottom) for different bandit algorithms.

Table 3: Total number of edges visited across 5 runs with horizon  $T = 200$  on Luxembourg B and Monaco.

Model	Luxembourg B		Monaco	
	BUCB	TS	BUCB	TS
BI	1941	1424	868	415
GP	810	772	547	385

In Fig. 4, the random regrets of BUCB and TS in the two real-world networks are illustrated. In general, we observe almost the same relative order as before but the BUCB models have swapped order. On the Luxembourg B network, we again observe that the regret of Bayes-GP-UCB starts to diverge around time step 100. The TS models have a significant gap between them on Luxembourg B. On the Monaco network, we observe the random regret is almost linear for all models at the end. This could be because the estimated cost of the most energy-efficient route is underestimated or because the models do not consistently identify and select the optimal route. Additionally, in multiple time steps, we observe that BI-TS has spikes in random regret. The inability of the Bayesian inference model to use the correlation between the edges could lead it to explore inefficient routes that the GP model avoids.

In Fig. 5, the explored routes for the two bandit algorithms with the GP model are visualized. At a quick glance, both algorithms explore a similar amount of the network. However, upon closer inspection, the BUCB algorithm seems to explore a couple of longer routes which TS does not. In both scenarios, TS identifies a preferred route that is run most frequently and where only minor deviations are tested. BUCB partially finds a preferred route but attempts two or more variants in equal proportions.

In Table 3, the total number of edges visited for the two bandit algorithms is presented. For both the Bayesian inference and GP models, BUCB tries more edges than the equivalent TS model. Similarly, the GP models try less edges than the equivalent Bayesian inference models.

### 5.3.2 Investigation of kernel design

To study an effective kernel function for the GP, we compare the 5 kernels introduced in Section 4.4.1 on the synthetic road network, and then compare a subset of them on the Luxembourg A and Monaco networks.

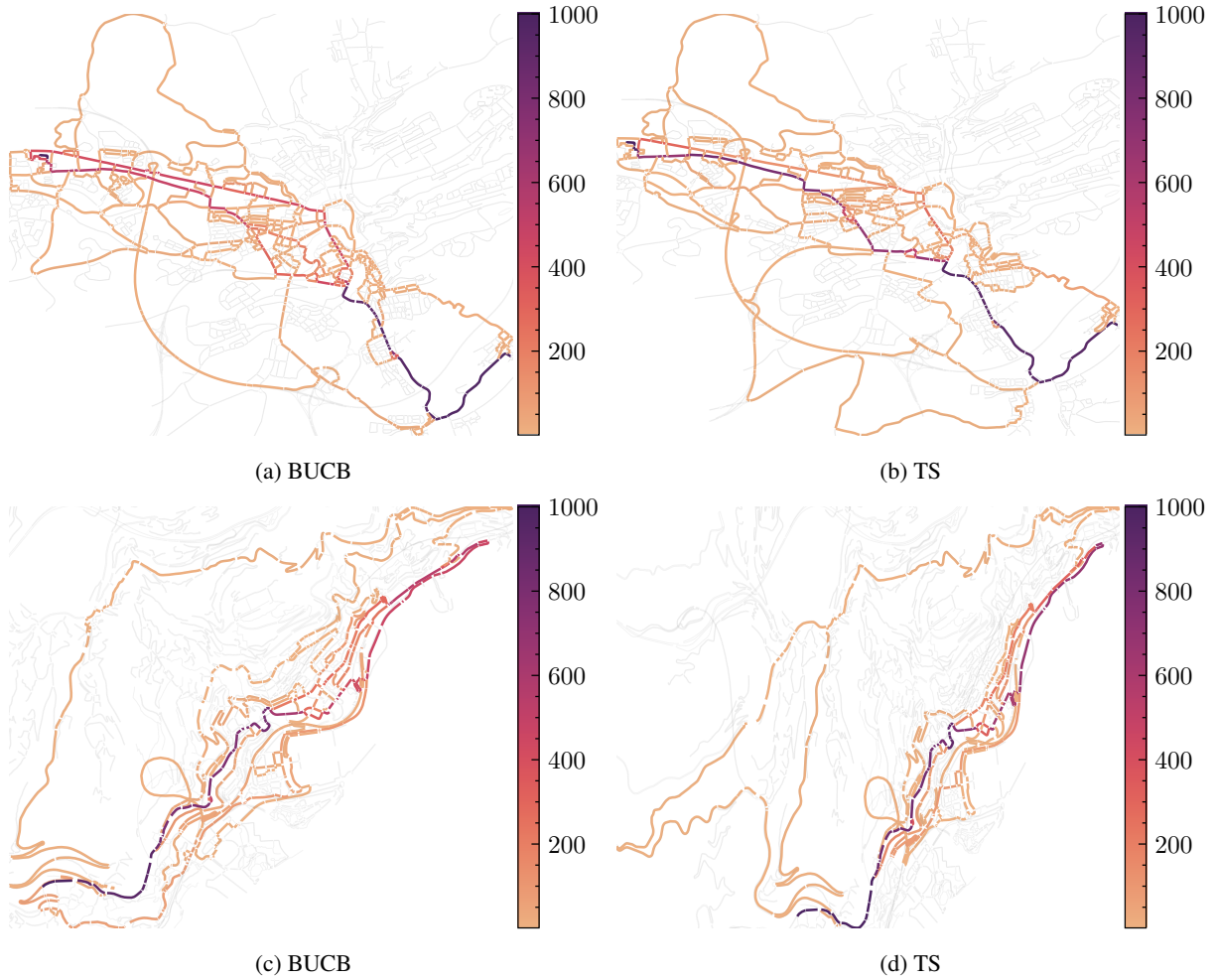


Figure 5: All selected routes across 5 runs on Luxembourg B and Monaco with the GP model using different bandit algorithms.

Table 4: Average total energy consumption (kWh) at  $t = 200$  on Luxembourg A.

Kernel	Luxembourg A	Monaco
$k_f$	$279.14 \pm 1.19$	$49.89 \pm 1.12$
$k_{G+f}$	$278.71 \pm 2.25$	$49.58 \pm 1.16$
$k_{G.f+f}$	$270.48 \pm 2.14$	$51.71 \pm 0.95$

The GP model is run with each kernel on the synthetic road network 10 times with a horizon of  $T = 1000$  using Algorithms 1 and 3. The Bayesian inference method described in Section 4.3 is used as a baseline. The cumulative regret for the kernels and the Bayesian baseline is shown in Fig. 6. The results indicate that the kernels  $k_{G.f+f}$ ,  $k_f$  and  $k_{G+f}$  improve upon the baseline. The kernels  $k_{G.f}$  and  $k_G$  have lower regret than the Bayesian inference model initially but fail to converge to a stable route in the end leading to accelerating cumulative regret.

To verify that the three well-performing kernels on the synthetic network ( $k_{G.f+f}$ ,  $k_f$ , and  $k_{G+f}$ ) also perform well on a simulated network, Algorithm 1 is applied 5 times on Luxembourg A and Monaco with a horizon of  $T = 200$ . The results are shown in Fig. 7. Finally, the total energy consumption is reported in Table 4 to contextualize the scale of the estimated regret and random regret.

From Fig. 7, the kernel  $k_{G.f+f}$  has significantly lower random regret than the other kernels on Luxembourg A. In the Monaco network,  $k_f$  and  $k_{G+f}$  has lower random regret than  $k_{G.f+f}$  but by a smaller margin. From Table 4, the difference in total energy consumption between the kernels  $k_f$  and  $k_{G.f+f}$  corresponds to a 3% reduction in

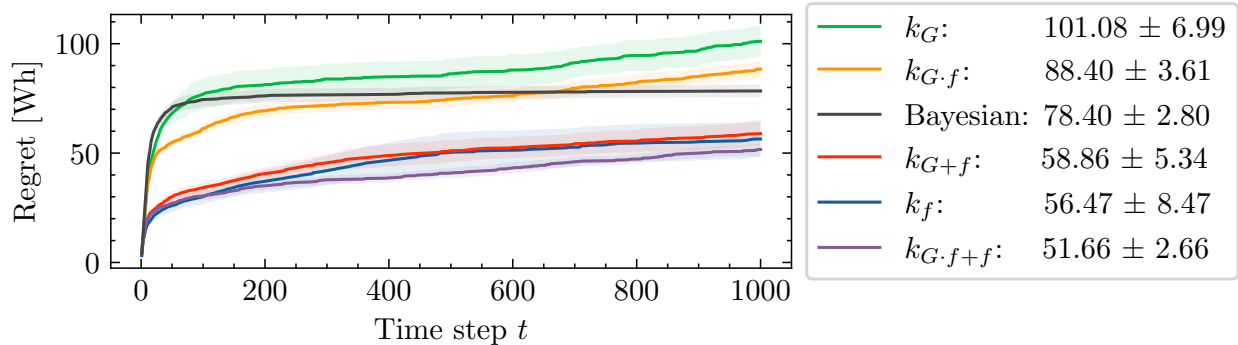


Figure 6: Cumulative regret on the synthetic road network for different kernels.

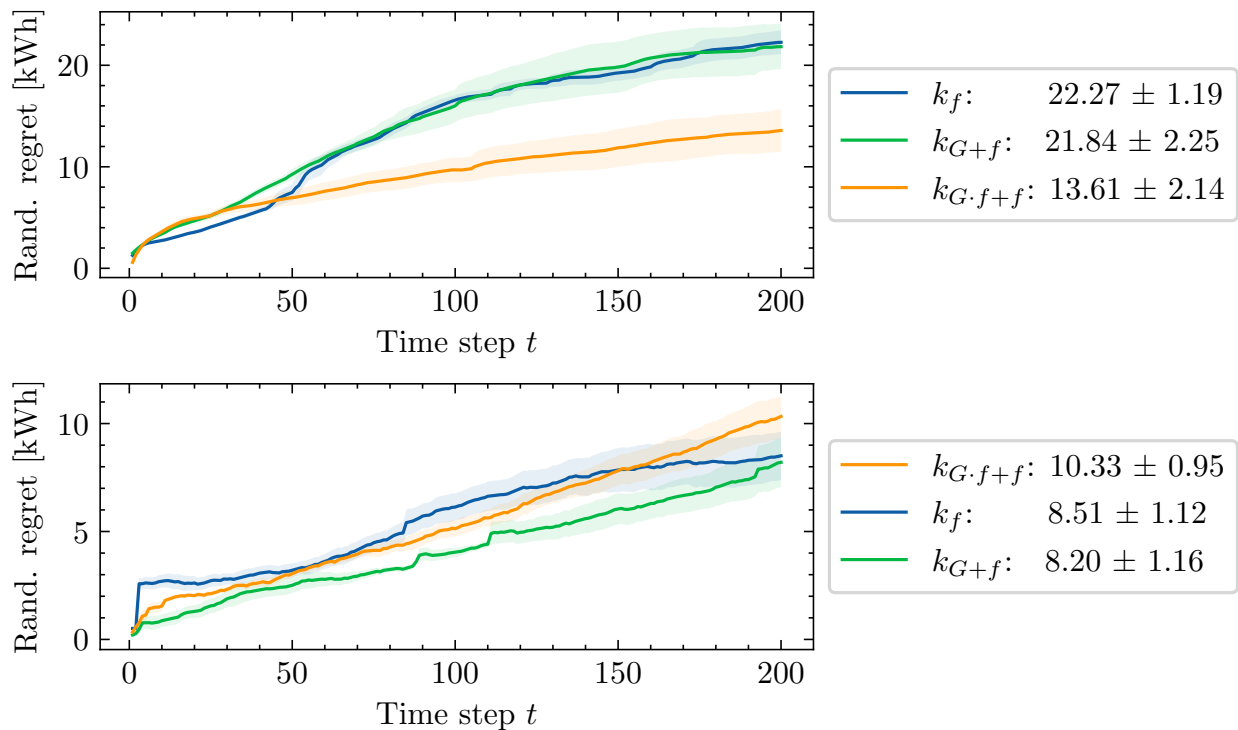


Figure 7: Random regret on Luxembourg A (top) and Monaco (bottom) for 3 promising kernels.



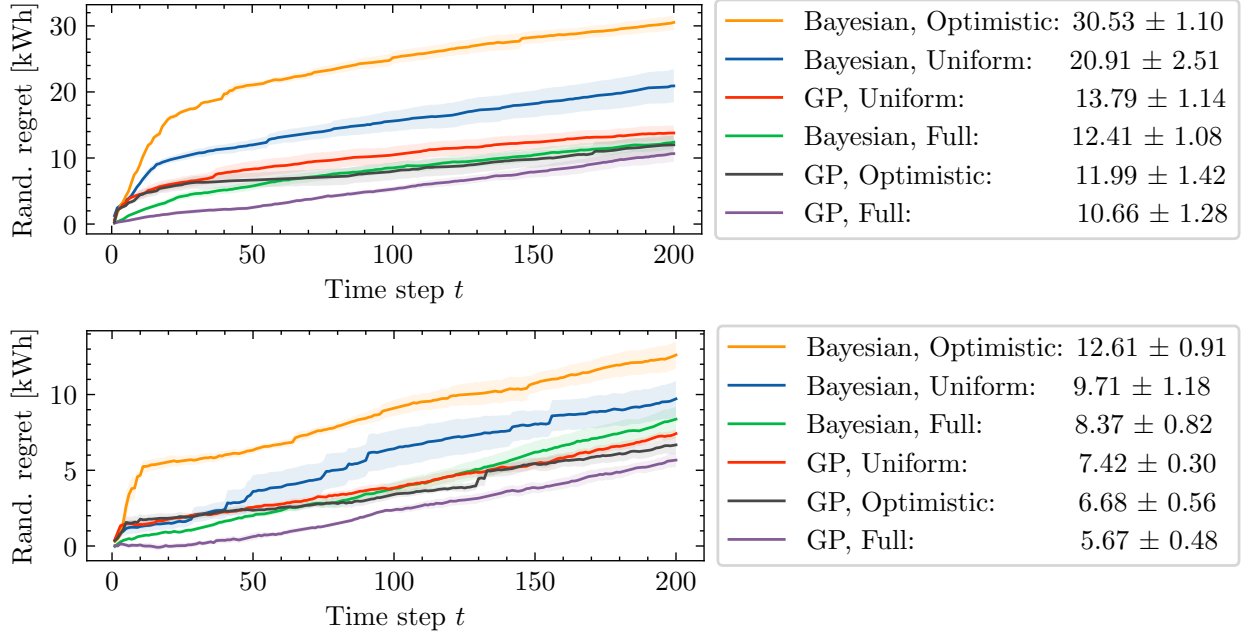


Figure 8: Random regret for the GP and Bayesian inference model using the three priors, Optimistic, Uniform and Full, in Luxembourg A (top) and Monaco (bottom).

energy consumption over 200 time steps on Luxembourg A. On the Monaco network, the difference in total energy consumption between  $k_{G+f}$  and  $k_{G.f+f}$  is 4%.

### 5.3.3 Investigation of prior distribution

To study the impact of priors on the GPs' performance and exploration, we test the three priors on Luxembourg A and Monaco. As before, we use the Bayesian inference method as a baseline to understand the difference in exploration between the GP and the baseline.

The random regret in both evaluation routes is illustrated in Fig. 8. The optimistic Bayesian model has the significantly highest random regret in both scenarios. The GP models, including the full prior, have lower random regret than the Bayesian baseline with corresponding prior in both scenarios. For the Bayesian baselines, priors with more information perform better. However, for the GP model, the optimistic prior achieves lower random regret than the uniform prior in both scenarios by a small margin. For both methods, the full prior yields the best results.

To better understand the impact of the priors, we visualize the chosen routes across all runs for each combination of prior and model. The chosen routes in Luxembourg A and Monaco are shown in Fig. 9 and Fig. 10, respectively. The visualizations are cropped to only show the selected routes. In addition, the total number of visited edges for the combinations of priors and models are reported in Table 5.

In Luxembourg A, we observe that the Bayesian models explore more than the GP models with an equivalent prior. The Bayesian model with optimistic prior explores the most and selects long routes (or detours) that are unlikely to be energy-efficient simply due to their length. Comparatively, the optimistic GP model does not explore excessively. The uniform Bayesian model also explores large parts of the network that seem unpromising, but to a lesser degree. In both Fig. 9 and Table 5, we observe that the exploration of the uniform GP model is very similar to the optimistic GP with only minor differences in Luxembourg A. With the full prior, the difference in exploration between the GP and Bayesian model is similar. Still, a close inspection reveals that the Bayesian model explores parts of the network that the GP model does not, which is evident from Table 5. Using the full prior helps both models focus on exploring the most promising routes in the network. The most frequently driven route is almost identical for all six models, with only minor deviations.

In Monaco, the same general patterns are observed. The Bayesian models explore more and all models explore less when the priors are more informative. The GP and Bayesian model with full prior explore only central Monaco and

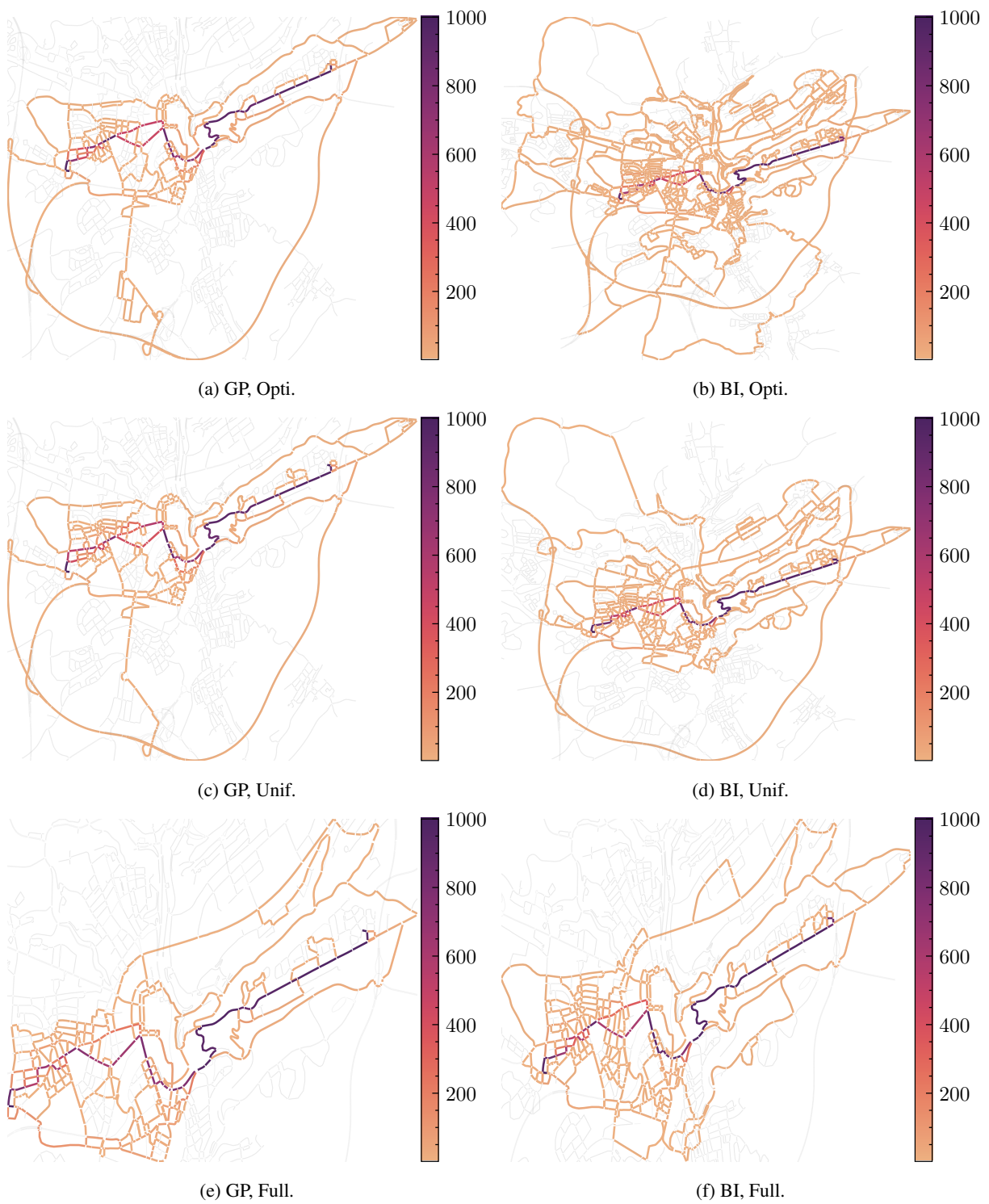


Figure 9: All selected routes across 5 runs on Luxembourg A with the GP and Bayesian inference models using different priors. Edges are colored based on the number of traversals.

Table 5: Total number of edges visited across 5 runs with horizon  $T = 200$  on Luxembourg A and Monaco.

Model	Luxembourg A, Prior			Monaco, Prior		
	Opti.	Unif.	Full	Opti.	Unif.	Full
Bayesian	1697	996	716	522	464	388
GP	526	519	496	444	365	288

avoid the northwestern hills. However, the full Bayesian model still explores the central region excessively and is unable to achieve lower estimated regret than the GP with optimistic and uniform priors.

## 5.4 Discussion

In this section, we discuss the experimental results, the methodology, and the proposed Gaussian process framework.

### 5.4.1 Bandit algorithm

In Section 5.3.1, the results showed that Thompson sampling achieves lower random regret compared to Bayes-UCB, which is consistent with other empirical studies on bandit problems comparing TS with UCB [55, 56, 28]. The difference in random regret between the two bandit algorithms increased steadily in both road networks. Inspecting the selected routes and the number of edges explored, Bayes-UCB explores more and does not converge to a single route as quickly as Thompson sampling. Therefore, according to the experimental results, the choice of bandit algorithm impacts the performance of the GP model, and Thompson sampling is the favorable algorithm.

### 5.4.2 Kernel design

The results in Section 5.3.2 demonstrate that the feature kernel combined with the graph kernel can efficiently learn to find energy-efficient routes. In the synthetic road network, the feature kernel is shown to be critical, whereas the combined feature and graph kernel  $k_{G.f+f}$  yields a small improvement.

The graph kernel requires discrete inputs which introduces difficulties in the optimization of the inducing points. Our approach in Algorithm 3 is to set the inducing points (edge index and features) to the top  $M$  most frequently visited edges and then optimize the feature dimensions of the inducing points using natural gradient descent. The benefit of this heuristic approach is that the discrete inducing dimension is set to relevant edges. However, this is potentially a limiting heuristic that could

1. make the predictions unstable if the most frequently visited edges shift too often,
2. reset the progress of continuous inducing feature optimization, and,
3. cluster the inducing points too close in the graph.

From Tables 3 and 5, the GP model did not explore more edges than the number of inducing points and the risk of first two issues should be limited - but this may not be true for much larger networks.

Work such as [57] propose and investigate methods of optimizing discrete inducing points. Since we only consider static features of the edges, the features and inducing points could be considered completely discrete. Applying the methods of [57] may provide a more elegant optimization scheme. When only using the feature kernel, the heuristic is not necessary. Removing the heuristic and only optimizing the inducing points could improve the results of the feature kernel.

In [41], the graph kernels were used to estimate the average speed on segments of the road network. In our GP model, we combine a graph and feature kernel to estimate energy consumption instead. Another usage of the graph kernel could be to estimate the average speed based on observed speeds of our vehicle and then feed the estimated speed to the feature kernel. The graph kernel assumes that the road segments in close proximity have similar energy consumption. By instead estimating the average speed with the graph kernel, we make the more reasonable assumption that road segments in close proximity have similar relative speeds or congestion levels.

The feature kernel was also only given the length, speed limit and incline as features. Additional features such as number of lanes, curvature or presence of traffic lights could also improve the feature kernel and allow it to emulate the graph kernel. We postpone the investigation of the importance of these different feature to future work.

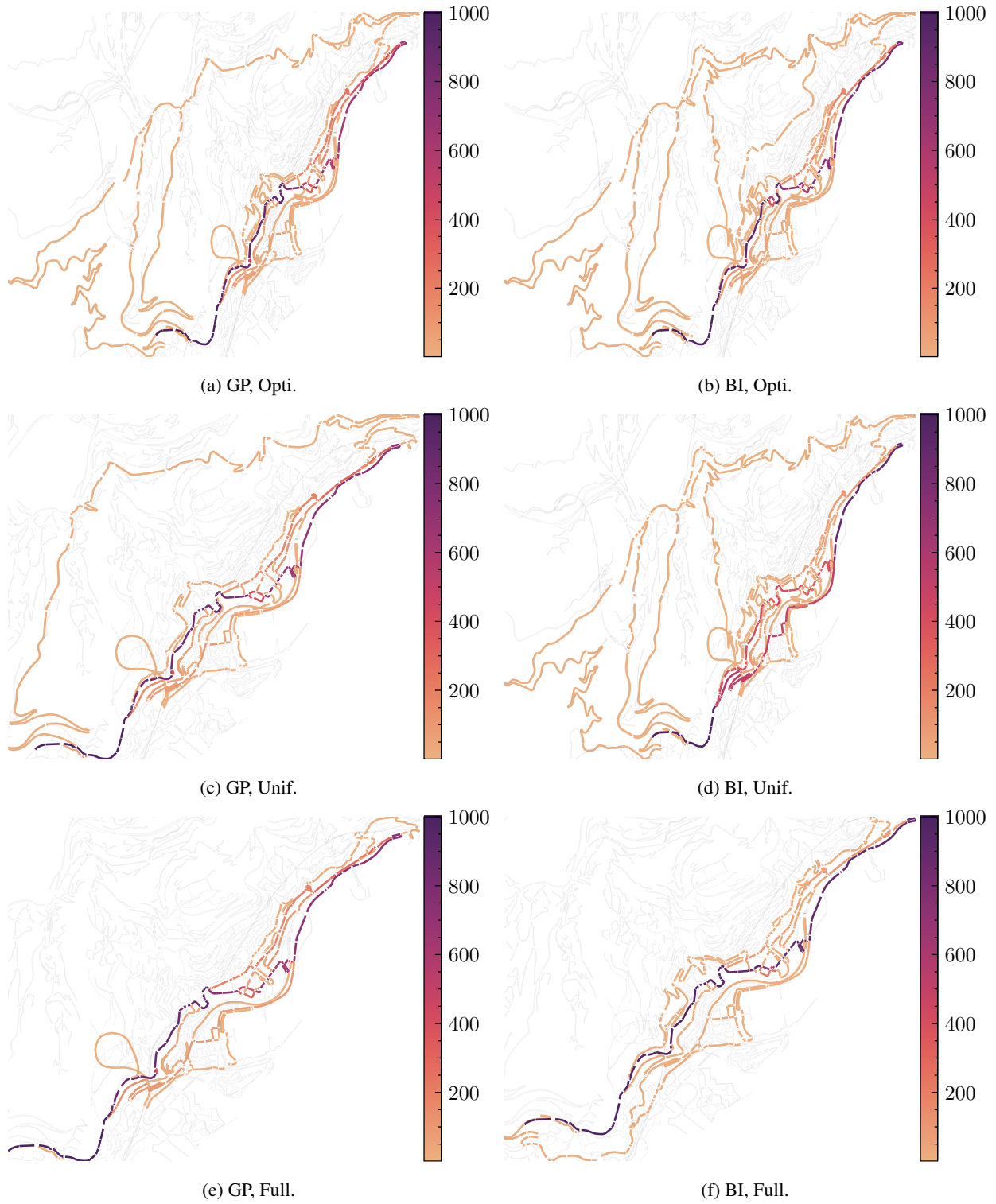


Figure 10: All selected routes across 5 runs on Monaco with the GP and Bayesian inference models using different priors. Edges are colored based on the number of traversals.

### 5.4.3 Informative prior

The results in Section 5.3.3 demonstrate that the GP model achieves lower random regret than the Bayesian inference model regardless of the prior. When the prior is uninformative and misleading (such as the optimistic prior), the GP model learns quickly through correlations using the kernel function. The kernel function’s length-scale parameter  $\ell_f$  was initialized as 1 for each feature, which is a relatively large value when using standardized features. With a smaller length scale, the GP model would extrapolate less and revert to the mean faster, which could lead to a higher exploration rate.

Naturally, the relative amount of information gained from using the features (kernel) decreases when using a more informative prior. This can be observed on Luxembourg A, where the difference in random regret between the GP and Bayesian inference model decreases as the prior becomes more informative.

For the GP model, the optimistic prior has lower random regret than the uniform prior in both scenarios. The two priors explore almost the same number of edges in Luxembourg A, but the uniform prior explores significantly less in Monaco. It is unclear why the uniform prior performs worse for the GP model.

## 6 Conclusion

We presented novel Bayesian regret bounds for the combinatorial Gaussian process semi-bandit with time-varying arm availability for three GP-based bandit algorithms: GP-UCB, Bayes-GP-UCB and GP-TS. Additionally, we experimentally evaluated the bandit algorithms on the online energy-efficient navigation problem on real-world and synthetic networks. We found that the proposed contextual Gaussian process model obtained lower regret than the non-contextual Bayesian inference model. Finally, the results showed that Thompson sampling performed better than Bayes-UCB for both the GP and Bayesian inference models.

## Acknowledgments

This work of Jack Sandberg and Morteza Haghiri Chehreghani was partially supported by the Wallenberg AI, Autonomous Systems and Software Program (WASP) funded by the Knut and Alice Wallenberg Foundation. The work of Niklas Åkerblom was partially funded by the Strategic Vehicle Research and Innovation Programme (FFI) of Sweden, through the project EENE (reference number: 2018-01937).

## References

- [1] Herbert Robbins. Some aspects of the sequential design of experiments. *Herbert Robbins Selected Papers*, pages 169–177, 1985.
- [2] Richard S. Sutton and Andrew G. Barto. *Reinforcement learning: an introduction*. Adaptive computation and machine learning series. The MIT Press, Cambridge, Massachusetts, second edition edition, 2018. ISBN 978-0-262-03924-6.
- [3] Yi Gai, Bhaskar Krishnamachari, and Rahul Jain. Combinatorial Network Optimization With Unknown Variables: Multi-Armed Bandits With Linear Rewards and Individual Observations. *IEEE/ACM Transactions on Networking*, 20(5):1466–1478, October 2012. ISSN 1558-2566. doi: 10.1109/TNET.2011.2181864. Conference Name: IEEE/ACM Transactions on Networking.
- [4] Nicolò Cesa-Bianchi and Gábor Lugosi. Combinatorial bandits. *Journal of Computer and System Sciences*, 78(5):1404–1422, September 2012. ISSN 0022-0000. doi: 10.1016/j.jcss.2012.01.001. URL <https://www.sciencedirect.com/science/article/pii/S0022000012000219>.
- [5] Wei Chen, Yajun Wang, and Yang Yuan. Combinatorial Multi-Armed Bandit: General Framework and Applications. In *Proceedings of the 30th International Conference on Machine Learning*, pages 151–159. PMLR, February 2013. URL <https://proceedings.mlr.press/v28/chen13a.html>. ISSN: 1938-7228.
- [6] Jean-Yves Audibert, Sébastien Bubeck, and Gábor Lugosi. Minimax Policies for Combinatorial Prediction Games. In *Proceedings of the 24th Annual Conference on Learning Theory*, pages 107–132. JMLR Workshop and Conference Proceedings, December 2011. URL <https://proceedings.mlr.press/v19/audibert11a.html>. ISSN: 1938-7228.
- [7] Lihong Li, Wei Chu, John Langford, and Robert E. Schapire. A contextual-bandit approach to personalized news article recommendation. In *Proceedings of the 19th international conference on World wide web, WWW ’10*, pages

- 661–670, New York, NY, USA, April 2010. Association for Computing Machinery. ISBN 978-1-60558-799-8. doi: 10.1145/1772690.1772758. URL <https://dl.acm.org/doi/10.1145/1772690.1772758>.
- [8] Andreas Krause and Cheng Ong. Contextual Gaussian Process Bandit Optimization. In *Advances in Neural Information Processing Systems*, volume 24. Curran Associates, Inc., 2011. URL [https://papers.nips.cc/paper\\_files/paper/2011/hash/f3f1b7fc5a8779a9e618e1f23a7b7860-Abstract.html](https://papers.nips.cc/paper_files/paper/2011/hash/f3f1b7fc5a8779a9e618e1f23a7b7860-Abstract.html).
- [9] Alekh Agarwal, Daniel Hsu, Satyen Kale, John Langford, Lihong Li, and Robert Schapire. Taming the Monster: A Fast and Simple Algorithm for Contextual Bandits. In *Proceedings of the 31st International Conference on Machine Learning*, pages 1638–1646. PMLR, June 2014. URL <https://proceedings.mlr.press/v32/agarwalb14.html>. ISSN: 1938-7228.
- [10] Li Zhou. A Survey on Contextual Multi-armed Bandits, February 2016. URL <http://arxiv.org/abs/1508.03326>. arXiv:1508.03326 [cs].
- [11] Niranjan Srinivas, Andreas Krause, Sham M. Kakade, and Matthias W. Seeger. Information-Theoretic Regret Bounds for Gaussian Process Optimization in the Bandit Setting. *IEEE Transactions on Information Theory*, 58(5):3250–3265, May 2012. ISSN 1557-9654. doi: 10.1109/TIT.2011.2182033. Conference Name: IEEE Transactions on Information Theory.
- [12] Daniel Russo and Benjamin Van Roy. Learning to Optimize via Posterior Sampling. *Mathematics of Operations Research*, April 2014. doi: 10.1287/moor.2014.0650. URL <https://pubsonline.informs.org/doi/abs/10.1287/moor.2014.0650>. Publisher: INFORMS.
- [13] William R Thompson. On the likelihood that one unknown probability exceeds another in view of the evidence of two samples. *Biometrika*, 25(3-4):285–294, December 1933. ISSN 0006-3444. doi: 10.1093/biomet/25.3-4.285. URL <https://doi.org/10.1093/biomet/25.3-4.285>.
- [14] Shion Takeno, Yu Inatsu, and Masayuki Karasuyama. Randomized Gaussian Process Upper Confidence Bound with Tighter Bayesian Regret Bounds. In *Proceedings of the 40th International Conference on Machine Learning*, pages 33490–33515. PMLR, July 2023. URL <https://proceedings.mlr.press/v202/takeno23a.html>. ISSN: 2640-3498.
- [15] Lijing Qin, Shouyuan Chen, and Xiaoyan Zhu. Contextual Combinatorial Bandit and its Application on Diversified Online Recommendation. In *Proceedings of the 2014 SIAM International Conference on Data Mining (SDM)*, Proceedings, pages 461–469. Society for Industrial and Applied Mathematics, April 2014. doi: 10.1137/1.9781611973440.53. URL <https://epubs.siam.org/doi/abs/10.1137/1.9781611973440.53>.
- [16] Lixing Chen, Jie Xu, and Zhuo Lu. Contextual Combinatorial Multi-armed Bandits with Volatile Arms and Submodular Reward. In *Advances in Neural Information Processing Systems*, volume 31. Curran Associates, Inc., 2018. URL [https://proceedings.neurips.cc/paper\\_files/paper/2018/hash/207f88018f72237565570f8a9e5ca240-Abstract.html](https://proceedings.neurips.cc/paper_files/paper/2018/hash/207f88018f72237565570f8a9e5ca240-Abstract.html).
- [17] Andi Nika, Sepehr Elahi, and Cem Tekin. Contextual Combinatorial Volatile Multi-armed Bandit with Adaptive Discretization. In *Proceedings of the Twenty Third International Conference on Artificial Intelligence and Statistics*, pages 1486–1496. PMLR, June 2020. URL <https://proceedings.mlr.press/v108/nika20a.html>. ISSN: 2640-3498.
- [18] Andi Nika, Sepehr Elahi, and Cem Tekin. Contextual Combinatorial Bandits with Changing Action Sets via Gaussian Processes, October 2022. URL <http://arxiv.org/abs/2110.02248>. arXiv:2110.02248 [cs, stat].
- [19] Sepehr Elahi, Baran Atalar, Sevda Ögüt, and Cem Tekin. Contextual Combinatorial Multi-output GP Bandits with Group Constraints. *Transactions on Machine Learning Research*, January 2023. ISSN 2835-8856. URL <https://openreview.net/forum?id=OqbGu3hdQb>.
- [20] Alessandro Nuara, Francesco Trovò, Nicola Gatti, and Marcello Restelli. A Combinatorial-Bandit Algorithm for the Online Joint Bid/Budget Optimization of Pay-per-Click Advertising Campaigns. *Proceedings of the AAAI Conference on Artificial Intelligence*, 32(1), April 2018. ISSN 2374-3468. doi: 10.1609/aaai.v32i1.11888. URL <https://ojs.aaai.org/index.php/AAAI/article/view/11888>. Number: 1.
- [21] Baihan Lin and Djallel Bouneffouf. Optimal Epidemic Control as a Contextual Combinatorial Bandit with Budget. In *2022 IEEE International Conference on Fuzzy Systems (FUZZ-IEEE)*, pages 1–8, July 2022. doi: 10.1109/FUZZ-IEEE55066.2022.9882725. URL <https://ieeexplore.ieee.org/document/9882725>. ISSN: 1558-4739.
- [22] Fang Shi, Weiwei Lin, Lisheng Fan, Xiaozhi Lai, and Xiumin Wang. Efficient Client Selection Based on Contextual Combinatorial Multi-Arm Bandits. *IEEE Transactions on Wireless Communications*, 22(8):5265–5277, August 2023. ISSN 1558-2248. doi: 10.1109/TWC.2022.3232891. URL <https://ieeexplore.ieee.org/document/10011209>. Conference Name: IEEE Transactions on Wireless Communications.

- [23] Emilie Kaufmann, Olivier Cappe, and Aurelien Garivier. On Bayesian Upper Confidence Bounds for Bandit Problems. In *Proceedings of the Fifteenth International Conference on Artificial Intelligence and Statistics*, pages 592–600. PMLR, March 2012. URL <https://proceedings.mlr.press/v22/kaufmann12.html>. ISSN: 1938-7228.
- [24] Andreas Artmeier, Julian Haselmayr, Martin Leucker, and Martin Sachenbacher. The Shortest Path Problem Revisited: Optimal Routing for Electric Vehicles. In Rüdiger Dillmann, Jürgen Beyerer, Uwe D. Hanebeck, and Tanja Schultz, editors, *KI 2010: Advances in Artificial Intelligence*, Lecture Notes in Computer Science, pages 309–316, Berlin, Heidelberg, 2010. Springer. ISBN 978-3-642-16111-7. doi: 10.1007/978-3-642-16111-7\_35.
- [25] Martin Sachenbacher, Martin Leucker, Andreas Artmeier, and Julian Haselmayr. Efficient energy-optimal routing for electric vehicles. In *Twenty-fifth AAAI conference on artificial intelligence*, 2011.
- [26] Jacob Holden, Nicholas Reinicke, and Jeff Cappellucci. Routee: A vehicle energy consumption prediction engine. *SAE International Journal of Advances and Current Practices in Mobility*, 2(2020-01-0939):2760–2767, 2020. doi: 10.4271/2020-01-0939. URL <https://www.sae.org/content/2020-01-0939/>.
- [27] Aaron Brooker, Jeffrey Gonder, Lijuan Wang, Eric Wood, Sean Lopp, and Laurie Ramroth. Fastsim: A model to estimate vehicle efficiency, cost and performance. Technical report, SAE Technical Paper, 2015. URL <https://www.sae.org/content/2015-01-0973/>.
- [28] Niklas Åkerblom, Yuxin Chen, and Morteza Haghiri Chehreghani. Online learning of energy consumption for navigation of electric vehicles. *Artificial Intelligence*, 317:103879, April 2023. ISSN 0004-3702. doi: 10.1016/j.artint.2023.103879. URL <https://www.sciencedirect.com/science/article/pii/S0004370223000255>.
- [29] Sayak Ray Chowdhury and Aditya Gopalan. On Kernelized Multi-armed Bandits. In *Proceedings of the 34th International Conference on Machine Learning*, pages 844–853. PMLR, July 2017. URL <https://proceedings.mlr.press/v70/chowdhury17a.html>. ISSN: 2640-3498.
- [30] Sattar Vakili, Kia Khezeli, and Victor Picheny. On Information Gain and Regret Bounds in Gaussian Process Bandits. In *Proceedings of The 24th International Conference on Artificial Intelligence and Statistics*, pages 82–90. PMLR, March 2021. URL <https://proceedings.mlr.press/v130/vakili21a.html>. ISSN: 2640-3498.
- [31] Kirthevasan Kandasamy, Akshay Krishnamurthy, Jeff Schneider, and Barnabas Póczos. Parallelised Bayesian Optimisation via Thompson Sampling. In *Proceedings of the Twenty-First International Conference on Artificial Intelligence and Statistics*, pages 133–142. PMLR, March 2018. URL <https://proceedings.mlr.press/v84/kandasamy18a.html>. ISSN: 2640-3498.
- [32] Biswajit Paria, Kirthevasan Kandasamy, and Barnabás Póczos. A Flexible Framework for Multi-Objective Bayesian Optimization using Random Scalarizations. In *Proceedings of The 35th Uncertainty in Artificial Intelligence Conference*, pages 766–776. PMLR, August 2020. URL <https://proceedings.mlr.press/v115/paria20a.html>. ISSN: 2640-3498.
- [33] Subhashis Ghosal and Anindya Roy. Posterior consistency of Gaussian process prior for nonparametric binary regression. *The Annals of Statistics*, 34(5), October 2006. ISSN 0090-5364. doi: 10.1214/009053606000000795. URL <http://arxiv.org/abs/math/0702686>. arXiv:math/0702686.
- [34] Michael L. Stein. *Interpolation of Spatial Data*. Springer Series in Statistics. Springer, New York, NY, 1999. ISBN 978-1-4612-7166-6 978-1-4612-1494-6. doi: 10.1007/978-1-4612-1494-6. URL <http://link.springer.com/10.1007/978-1-4612-1494-6>.
- [35] Seok-Ho Chang, Pamela C. Cosman, and Laurence B. Milstein. Chernoff-Type Bounds for the Gaussian Error Function. *IEEE Transactions on Communications*, 59(11):2939–2944, 2011. doi: 10.1109/TCOMM.2011.072011.100049.
- [36] Dijkstra E. W. A Note on Two Problems in Connexion with Graphs. *Numerische Mathematik*, 1:269–271, 1959. URL <https://cir.nii.ac.jp/crid/1571698600523742592>.
- [37] Alfonso Shimbel. Structure in communication nets. *Proceedings of the Symposium on Information Networks*, pages 119–203, 1954. URL <https://cir.nii.ac.jp/crid/1573950399431729664>. Publisher: Polytechnic Institute of Brooklyn.
- [38] Richard Bellman. On a routing problem. *Quarterly of Applied Mathematics*, 16(1):87–90, 1958. ISSN 0033-569X, 1552-4485. doi: 10.1090/qam/102435. URL <https://www.ams.org/qam/1958-16-01/S0033-569X-1958-0102435-2/>.
- [39] L. R. Ford. Network Flow Theory. Technical report, RAND Corporation, January 1956. URL <https://www.rand.org/pubs/papers/P923.html>.

- [40] Andreas Bjorklund, Thore Husfeldt, and Sanjeev Khanna. Approximating longest directed paths and cycles. In *ICALP*, volume 3142, pages 222–233. Springer, 2004.
- [41] Viacheslav Borovitskiy, Iskander Azangulov, Alexander Terenin, Peter Mostowsky, Marc Deisenroth, and Nicolas Durrande. Matérn Gaussian Processes on Graphs. In Arindam Banerjee and Kenji Fukumizu, editors, *Proceedings of The 24th International Conference on Artificial Intelligence and Statistics*, volume 130 of *Proceedings of Machine Learning Research*, pages 2593–2601. PMLR, April 2021. URL <https://proceedings.mlr.press/v130/borovitskiy21a.html>.
- [42] Michalis Titsias. Variational Learning of Inducing Variables in Sparse Gaussian Processes. In *Proceedings of the Twelfth International Conference on Artificial Intelligence and Statistics*, pages 567–574. PMLR, April 2009. URL <https://proceedings.mlr.press/v5/titsias09a.html>. ISSN: 1938-7228.
- [43] James Hensman, Nicolò Fusi, and Neil D. Lawrence. Gaussian Processes for Big Data. In *Proceedings of the Twenty-Ninth Conference on Uncertainty in Artificial Intelligence*, UAI’13, pages 282–290, Arlington, Virginia, USA, 2013. AUAI Press. event-place: Bellevue, WA.
- [44] Sattar Vakili, Henry Moss, Artem Artemev, Vincent Dutordoir, and Victor Picheny. Scalable Thompson Sampling using Sparse Gaussian Process Models. In *Advances in Neural Information Processing Systems*, volume 34, pages 5631–5643. Curran Associates, Inc., 2021. URL [https://proceedings.neurips.cc/paper\\_files/paper/2021/hash/2c7f9ccb5a39073e24babc3a4cb45e60-Abstract.html](https://proceedings.neurips.cc/paper_files/paper/2021/hash/2c7f9ccb5a39073e24babc3a4cb45e60-Abstract.html).
- [45] Hugh Salimbeni, Stefanos Eleftheriadis, and James Hensman. Natural Gradients in Practice: Non-Conjugate Variational Inference in Gaussian Process Models. In Amos Storkey and Fernando Perez-Cruz, editors, *Proceedings of the Twenty-First International Conference on Artificial Intelligence and Statistics*, volume 84 of *Proceedings of Machine Learning Research*, pages 689–697. PMLR, April 2018. URL <https://proceedings.mlr.press/v84/salimbeni18a.html>.
- [46] Diederik P. Kingma and Jimmy Ba. Adam: A Method for Stochastic Optimization. In Yoshua Bengio and Yann LeCun, editors, *3rd International Conference on Learning Representations, ICLR 2015, San Diego, CA, USA, May 7-9, 2015, Conference Track Proceedings*, 2015. URL <http://arxiv.org/abs/1412.6980>.
- [47] Nicholas Socci, Daniel Lee, and H. Sebastian Seung. The Rectified Gaussian Distribution. In *Advances in Neural Information Processing Systems*, volume 10. MIT Press, 1997. URL [https://papers.nips.cc/paper\\_files/paper/1997/hash/28fc2782ea7ef51c1104ccf7b9bea13d-Abstract.html](https://papers.nips.cc/paper_files/paper/1997/hash/28fc2782ea7ef51c1104ccf7b9bea13d-Abstract.html).
- [48] Markus Harva and Ata Kabán. Variational learning for rectified factor analysis. *Signal Processing*, 87(3):509–527, March 2007. ISSN 0165-1684. doi: 10.1016/j.sigpro.2006.06.006. URL <https://www.sciencedirect.com/science/article/pii/S0165168406002118>.
- [49] Maxime Beauchamp. On numerical computation for the distribution of the convolution of  $N$  independent rectified Gaussian variables. *Journal de la Société Française de Statistique*, 159(1):88–111, March 2018. ISSN 2102-6238. URL <http://journal-sfds.fr/article/view/669>. Number: 1.
- [50] Pablo Alvarez Lopez, Michael Behrisch, Laura Bieker-Walz, Jakob Erdmann, Yun-Pang Flötteröd, Robert Hilbrich, Leonhard Lücken, Johannes Rummel, Peter Wagner, and Evamarie Wiessner. Microscopic Traffic Simulation using SUMO. In *2018 21st International Conference on Intelligent Transportation Systems (ITSC)*, pages 2575–2582, November 2018. doi: 10.1109/ITSC.2018.8569938. ISSN: 2153-0017.
- [51] Lara Codeca and Jérôme Härrri. Monaco SUMO Traffic (MoST) Scenario: A 3D Mobility Scenario for Cooperative ITS. In *SUMO 2018, SUMO User Conference, Simulating Autonomous and Intermodal Transport Systems, May 14-16, 2018, Berlin, Germany*, Berlin, GERMANY, May 2018.
- [52] Lara Codeca, Raphael Frank, Sebastien Faye, and Thomas Engel. Luxembourg SUMO Traffic (LuST) Scenario: Traffic Demand Evaluation. *IEEE Intelligent Transportation Systems Magazine*, 9(2):52–63, 2017. ISSN 1941-1197. doi: 10.1109/MITS.2017.2666585. Conference Name: IEEE Intelligent Transportation Systems Magazine.
- [53] Administration de la navigation aérienne. Digital Terrain Model (high DEM resolution) - Portail Open Data, n.d. URL <https://data.public.lu/en/datasets/digital-terrain-model-high-dem-resolution/>.
- [54] QGIS Development Team. *QGIS Geographic Information System*. QGIS Association, 2023. URL <https://www.qgis.org>.
- [55] Olivier Chapelle and Lihong Li. An Empirical Evaluation of Thompson Sampling. In *Advances in Neural Information Processing Systems*, volume 24. Curran Associates, Inc., 2011. URL [https://papers.nips.cc/paper\\_files/paper/2011/hash/e53a0a2978c28872a4505bdb51db06dc-Abstract.html](https://papers.nips.cc/paper_files/paper/2011/hash/e53a0a2978c28872a4505bdb51db06dc-Abstract.html).



- [56] Siwei Wang and Wei Chen. Thompson Sampling for Combinatorial Semi-Bandits. In *Proceedings of the 35th International Conference on Machine Learning*, pages 5114–5122. PMLR, July 2018. URL <https://proceedings.mlr.press/v80/wang18a.html>. ISSN: 2640-3498.
- [57] Vincent Fortuin, Gideon Dresdner, Heiko Strathmann, and Gunnar Rätsch. Sparse Gaussian Processes on Discrete Domains. *IEEE Access*, 9:76750–76758, 2021. ISSN 2169-3536. doi: 10.1109/ACCESS.2021.3082761. Conference Name: IEEE Access.
- [58] K. B. Petersen and M. S. Pedersen. The Matrix Cookbook, November 2012. URL <http://www2.compute.dtu.dk/pubdb/pubs/3274-full.html>.

## A Notation

Table 6: Summary of notation.

Notation	Description
$\mathcal{A}$	Set of base arms.
$d$	Dimension of base arm space.
$\mathcal{S}$	Set of feasible super arms.
$\mathbf{a}$	Super-arm.
$a$	Base-arm.
$f(a)$	Expected reward for base arm $a$ .
$\mathcal{GP}(\mu, k)$	Gaussian process with mean $\mu(a)$ and covariance $k(a, a')$ .
$\mu(a)$	Prior mean of arm $a$ .
$k(a, a')$	Prior covariance between arms $a$ and $a'$ .
$t$	A time step.
$\mathcal{A}_t$	Base arms available at time $t$ .
$\mathbf{a}_t$	Superarm selected at time $t$ .
$\mathcal{S}_t$	Superarms available at time $t$ .
$K$	Maximum size of available superarms.
$\mathbf{r}_t$	Observed base arms rewards at time $t$ .
$r_{t,a}$	Observed base arm reward at time $t$ for base arm $a$ .
$\varepsilon$	Noise when observing a base arm.
$\zeta^2$	Noise variance of the base arms.
$R_t$	Total reward at time $t$ .
$T$	Time horizon.
$\boldsymbol{\theta}_0$	Prior agent parameters.
$\boldsymbol{\theta}_t$	Agent parameters at time $t$ .
$\mathbf{U}_t$	Base arm upper indices at time $t$ .
$H_t$	History of available arms, selected super-arms and observed rewards up to time $t$ .
$\mathbb{E}[\cdot]$	Expected value.
BayesRegret( $T$ )	Bayesian regret up to time $T$ .
$\mathbf{a}_t^*$	Optimal super-arm at time $t$ .
$f(\mathbf{a})$	Expected reward of super arm $\mathbf{a}$ .
$N$	Number of arms.
$\mathbf{f}$	Expected value of GP in finite subset
$N_{t-1}$	Total number of base arms selected up to, and including, time $t - 1$ .
$\mathbf{y}$	Vector of observed rewards for all selected base arms up to time $t - 1$ .
$\boldsymbol{\mu}$	Vector of prior expected rewards for all selected base arms up to time $t - 1$ .
$\mu_{t-1}(a)$	Posterior mean of arm $a$ at time $t - 1$ .
$k_{t-1}(a, a')$	Posterior covariance between arms $a$ and $a'$ at time $t - 1$ .
$\mathbf{K}$	Covariance matrix of the previously selected arms up to time $t - 1$ .
$\mathbf{k}(a)$	Vector of covariances between $a$ and the previously selected arms up to time $t - 1$ .
$I$	Identity matrix.
$\sigma_{t-1}(a)$	Posterior standard deviation of base arm $a$ at time $t - 1$ .
$\sigma_{t-1}^2(a)$	Posterior variance of base arm $a$ at time $t - 1$ .
$\mu_{t-1}(\mathbf{a})$	Sum of posterior mean for super arm $\mathbf{a}$ at time $t - 1$ .
$\sigma_{t-1}(\mathbf{a})$	Sum of posterior standard deviations for super arm $\mathbf{a}$ at time $t - 1$ .

Table 6 (continued)

Notation	Description
$\beta_t$	Confidence parameter at time $t$ of GP-UCB or Bayes-GP-UCB.
$\mathcal{O}(\cdot)$	Order of a function.
$\eta_t$	Quantile parameter of Bayes-GP-UCB.
$Q(p, \lambda)$	The $p$ -quantile of the distribution $\lambda$ .
$\lambda$	A generic distribution.
$\mathcal{N}(\mu, \sigma^2)$	Univariate normal distribution with mean $\mu$ and variance $\sigma^2$ .
$\text{erf}^{-1}$	Inverse of the error function.
$\hat{f}_t(a)$	Sample for base arm $a$ from the posterior distribution at time $t$ .
$\hat{f}_t(\mathbf{a})$	Sum of posterior samples over the base arms in the super arm $\mathbf{a}$ .
$\gamma_T$	Maximal information gain from $T$ samples.
$I(\mathbf{y}_{\mathbf{a}}; f)$	Mutual information between $\mathbf{y}_{\mathbf{a}}$ and $f$ .
$H(\cdot)$	Entropy of a random variable.
$k$	A kernel function.
$\nu$	Smoothness parameter of Matérn kernel.
$C_1$	Bounding radius of the base arm set.
$L$	Lipschitz constant.
$C_2$	First regularity parameter for sample derivatives in Assumption 1.
$C_3$	Second regularity parameter for sample derivatives in Assumption 1.
$a^{(j)}$	$j$ -th element of base arm $a$ .
$l$	Lengthscale in Assumption 1.
$\mathcal{D}_t$	Discretization of base arm set at time $t$ .
$\tau_t$	Number of discrete points per dimension in $\mathcal{D}_t$ at time $t$ .
$[a]_{\mathcal{D}_t}$	Nearest point in $\mathcal{D}_t$ for base arm $a$ .
$[\mathbf{a}]_{\mathcal{D}_t}$	Set of nearest base arms in $\mathcal{D}_t$ for all base arms in $\mathbf{a}$ .
$C_4$	Simplifying constant dependent on the noise variance $\zeta^2$ .
$\omega$	First parameter in bounds on inverse error function.
$\vartheta$	Second parameter in bounds on inverse error function.
$\xi$	Quantile parameter growth rate.
$\mathbf{a}_t^*   H_t$	Optimal super arm at time $t$ given the history.
$\mathbf{a}_t   H_t$	Selected super arm at time $t$ given the history.
$\mathcal{V}$	Set of vertices in a graph or intersections of road segments in a road network.
$\mathcal{E}$	Set of edges in a graph or road segments in a road network.
$\mathcal{G}$	Graph/road network.
$e$	An edge in a graph.
$u$	A node in a graph.
$\mathcal{L}(\mathcal{G})$	Line graph of $\mathcal{G}$ .
$\mathcal{C}_t$	Set of connections available at time $t$ .
$c$	A connection between two edges.
$\mathcal{P}_t$	Set of paths from start node to end node at time $t$ .
$\mathbf{p}$	A path.
$x_{t,e}$	Context vector at time $t$ for each edge $e$ .
$\ell_e$	Length of edge $e$ .
$\alpha_e$	Inclination of edge $e$ .
$v_e$	Speed limit of edge $e$ .
$E_e^{\text{det}}$	Deterministic energy consumption model for edge $e$ .
$m$	Mass.
$C_r$	Rolling resistance.
$A$	Front surface area.
$C_d$	Air drag coefficient.
$\eta$	Powertrain efficiency.
$g$	Gravitational acceleration.
$\rho$	Air density.
$E_e$	Energy consumed when driving across edge $e$ .
$\mu_e^*$	True mean energy consumption of edge $e$ .
$(\zeta_e^*)^2$	True variance of the energy consumption of edge $e$ .

Table 6 (continued)

Notation	Description
$p(\cdot)$	Probability density function.
$\mathcal{N}(\cdot \mu, \sigma^2)$	Probability density function of a Gaussian with parameters $\mu$ and $\sigma^2$ .
$\mu_{e,0}$	Prior mean of the energy consumption for edge $e$ .
$\sigma_{e,0}^2$	Prior variance of the mean energy consumption for edge $e$ .
$\mu_{e,t}$	Posterior mean of the energy consumption for edge $e$ at time $t$ .
$\sigma_{e,t}^2$	Posterior variance of the mean energy consumption for edge $e$ at time $t$ .
$\mathbf{W}_{\mathcal{L}}$	Weight matrix of the line graph $\mathcal{L}(\mathcal{G})$ .
$W_{e_1, e_2}$	Weight between edge $e_1$ and $e_2$ .
$\bar{\ell}$	Average length of all edges $e$ .
$\ell_e$	Length of edge $e_1$ .
$\Delta_I$	Incidence graph Laplacian.
$\mathbf{B}$	Incidence matrix.
$B_{e,c}$	Incidence value between edge $e$ and connection $c$ .
$\mathbf{U}_I$	Eigenvectors of incidence graph Laplacian.
$\Lambda_I$	Matrix with eigenvalues of the incidence graph Laplacian on the diagonal.
$\kappa$	Scale parameter of the graph Matérn kernel.
$k_G$	Graph Matérn kernel.
$\sigma_G$	Outputscale parameter of the graph Matérn kernel.
$k_f$	Feature kernel.
$\sigma_f$	Outputscale parameter of the feature kernel.
$\ell_f$	Lengthscale vector for the feature kernel.
$x_e$	Feature vector of edge $e$ .
$D$	Feature distance between two edges.
$\text{diag}(\cdot)$	Matrix with diagonal defined by the input vector.
$k_{G+f}$	Kernel combining $k_G$ and $k_f$ through addition.
$k_{G \cdot f}$	Kernel combining $k_G$ and $k_f$ through multiplication.
$k_{G \cdot f + f}$	Kernel combining $k_G$ and two different $k_f$ through multiplication and addition.
$\mathbf{Z}_t$	Set of inducing points.
$z_i$	The $i$ -th inducing point.
$M$	Number of inducing points.
$q(\mathbf{u}_t)$	Prior distribution for inducing variables.
$\mathbf{u}_t$	Inducing variables.
$\mathbf{m}_t$	Mean of inducing variables.
$\mathcal{S}_t$	Covariance matrix of the inducing variables.
$B$	Batch size.
$\tilde{\mathbf{a}}$	Subsampled set of base arms.
$\tilde{\mathbf{r}}$	Subsampled set of base arm rewards.
$\zeta^2$	Heteroskedastic noise sample.
$U_{t,e}$	Edge weight at time $t$ of edge $e$ .
$\hat{\mu}_e$	Posterior estimate for edge $e$ .
$\mathcal{N}^R(\mu, \sigma^2)$	Rectified Gaussian distribution with parameters $\mu$ and $\sigma^2$ .
$\Phi(\cdot)$	Standard Gaussian cumulative probability function.
$\phi(\cdot)$	Standard Gaussian probability density function.
$E_{e,c}$	Cluster energy consumption for edge $e$ .
$\tilde{x}_e$	Horizontal coordinate for edge $e$ in the synthetic network.
$\tilde{y}_e$	Vertical coordinate for edge $e$ in the synthetic network.
$\tilde{x}_g$	Horizontal graph center coordinate in the synthetic network.
$\tilde{y}_g$	Vertical graph center coordinate in the synthetic network.
$\boldsymbol{\mu}_0$	Prior mean vector.
$\boldsymbol{\sigma}_0$	Vector of prior standard deviation of mean.
$s_0$	Prior standard deviation of noise.
$E_e^{\text{det}}$	Average of $E_e^{\text{det}}$ for all edges.
$\sigma^{\text{det}}$	Standard deviation of $E_e^{\text{det}}$ for all edges.
$\nu_G$	Smoothness parameter of the graph kernel.
$\kappa_G$	Scale parameter of the graph kernel.

Table 6 (continued)

Notation	Description
$\mathbf{r}^*$	Expected reward of optimal route.
$w_e^*$	True rectified weight of edge $e$ .
$\mathbf{p}^*$	Optimal path.
$\mathbf{p}_t$	Path selected at time $t$ .
$\hat{\mathbf{r}}$	Estimate of the negated energy consumption of optimal route.
$q$	Quantile level for the quantile coverage error.
$U_t(a, H_t)$	Upper confidence bound for base arm $a$ given the history $H_t$ , shorthand: $U_t(a)$ .
$L_t(a, H_t)$	Lower confidence bound for base arm $a$ given the history $H_t$ , shorthand: $L_t(a)$ .
$U_t(\mathbf{a}, H_t)$	Sum of upper confidence bounds for super arm $\mathbf{a}$ .
$L_t(\mathbf{a}, H_t)$	Sum of lower confidence bounds for super arm $\mathbf{a}$ .
$\mathbf{L}$	Cholesky decomposition of $\mathbf{K} + \zeta^2 I$ .
$\chi^2$	Chi-squared distribution.
$\text{eig}(\cdot)$	Set of eigenvalues of a square matrix.

## B Extended Regret Analysis

In the following sections, we include the proofs of the presented theorems and lemmas. Similar to previous work, we initially prove regret bounds for the finite case in Appendix B.1 and then use the finite case to prove the infinite case in Appendix B.2. Since the proofs for GP-UCB, Bayes-GP-UCB and GP-TS share most steps, the common steps have been separated into lemmas to better highlight when the proofs differ. In Appendix B.3, we provide lemmas to bound the inverse error function.

The proofs utilize upper and lower confidence bounds which are defined as follows for any base arm  $a \in \mathcal{A}$  and history  $H_t$ :

$$U_t(a, H_t) := \mu_{t-1}(a) + \sqrt{\beta_t} \sigma_{t-1}(a), \quad (28)$$

$$L_t(a, H_t) := \mu_{t-1}(a) - \sqrt{\beta_t} \sigma_{t-1}(a). \quad (29)$$

For any superarm  $\mathbf{a} \in \mathcal{S}$ , the confidence bounds are defined as the sum of base arm confidence bounds:

$$U_t(\mathbf{a}, H_t) := \sum_{a \in \mathbf{a}} U_t(a, H_t), \text{ and } L_t(\mathbf{a}, H_t) := \sum_{a \in \mathbf{a}} L_t(a, H_t). \quad (30)$$

When convenient, we drop  $H_t$  in the notation for  $U_t$  and  $L_t$  and treat them as random variables.

### B.1 Finite case

In this section, we state and prove the regret bounds in the finite case for the three bandit algorithms. To begin, we establish lemmas that demonstrate the general procedure for the proofs and later we combine the lemmas to get the desired regret bounds.

In the following lemma, the Bayesian regret is separated into two terms.

**Lemma 6.**

$$\text{BayesRegret}(T) \leq \sum_{t \in [T]} \mathbb{E}[f(\mathbf{a}_t^*) - U_t(\mathbf{a}_t^*)] + \sum_{t \in [T]} \mathbb{E}[U_t(\mathbf{a}_t) - f(\mathbf{a}_t)] \quad (31)$$

holds for any GP-UCB method and holds with equality for GP-TS.

*Proof.* The proof follows the procedure of [12, Prop. 1] for GP-TS and [14, Thm. B.1] for GP-UCB. For GP-TS,

$$\text{BayesRegret}(T) = \sum_{t \in [T]} \mathbb{E}[f(\mathbf{a}_t^*) - f(\mathbf{a}_t)] \quad (32)$$

$$= \sum_{t \in [T]} \mathbb{E}_{H_t} [\mathbb{E}_t [f(\mathbf{a}_t^*) - U_t(\mathbf{a}_t^*) + U_t(\mathbf{a}_t) - f(\mathbf{a}_t) | H_t]] \quad \left( \mathbf{a}_t^* | H_t \stackrel{d}{=} \mathbf{a}_t | H_t \right) \quad (33)$$

$$= \sum_{t \in [T]} \mathbb{E}[f(\mathbf{a}_t^*) - U_t(\mathbf{a}_t^*)] + \sum_{t \in [T]} \mathbb{E}[U_t(\mathbf{a}_t) - f(\mathbf{a}_t)]. \quad (34)$$

Similarly, for any GP-UCB method,

$$\text{BayesRegret}(T) = \sum_{t \in [T]} \mathbb{E}[f(\mathbf{a}_t^*) - f(\mathbf{a}_t)] \quad (35)$$

$$= \sum_{t \in [T]} \mathbb{E}[f(\mathbf{a}_t^*) - U_t(\mathbf{a}_t^*) + U_t(\mathbf{a}_t^*) - U_t(\mathbf{a}_t) + U_t(\mathbf{a}_t) - f(\mathbf{a}_t)] \quad (36)$$

$$\leq \sum_{t \in [T]} \mathbb{E}[f(\mathbf{a}_t^*) - U_t(\mathbf{a}_t^*) + U_t(\mathbf{a}_t) - f(\mathbf{a}_t)] \quad (37)$$

where the final step uses that  $U_t(\mathbf{a}_t^*) - U_t(\mathbf{a}_t) \leq 0$  since  $\mathbf{a}_t = \arg \max_{\mathbf{a} \in \mathcal{S}_t} U_t(\mathbf{a})$ .  $\square$

Whilst Lemma 6 applies to all the considered bandit algorithms, the two terms in the decomposition requires knowing the specific bandit algorithm. Bounding the left term requires knowledge of the confidence parameter  $\beta_t$ . Therefore we present a lemma that applies to GP-UCB and GP-TS, and another lemma that applies to Bayes-GP-UCB.

**Lemma 7.** *If  $|\mathcal{A}| < \infty$ , then*

$$\sum_{t \in [T]} \mathbb{E}[f(\mathbf{a}_t^*) - U_t(\mathbf{a}_t^*)] \leq \frac{\pi^2}{6} \quad (38)$$

*holds for GP-UCB and GP-TS with  $\beta_t = 2 \log(|\mathcal{A}|t^2/\sqrt{2\pi})$ .*

*Proof.* The proof closely follows the proof of [14, Thm. B.1]. Let  $R_1 = \sum_{t \in [T]} \mathbb{E}[f(\mathbf{a}_t^*) - U_t(\mathbf{a}_t^*)]$ , then

$$R_1 = \sum_{t \in [T]} \mathbb{E}_{H_t} [\mathbb{E}_t [f(\mathbf{a}_t^*) - U_t(\mathbf{a}_t^*) | H_t]] \quad (39)$$

$$= \sum_{t \in [T]} \mathbb{E}_{H_t} \left[ \mathbb{E}_t \left[ \sum_{a \in \mathbf{a}_t^*} f(a) - U_t(a) \middle| H_t \right] \right] \quad (40)$$

$$\leq \sum_{t \in [T]} \mathbb{E}_{H_t} \left[ \mathbb{E}_t \left[ \sum_{a \in \mathbf{a}_t^*} (f(a) - U_t(a))_+ \middle| H_t \right] \right] \quad ((x)_+ := \max(0, x) \geq x) \quad (41)$$

$$\leq \sum_{t \in [T]} \mathbb{E}_{H_t} \left[ \sum_{a \in \mathcal{A}} \mathbb{E}_t \left[ (f(a) - U_t(a))_+ \middle| H_t \right] \right]. \quad (\mathbf{a}_t^* \subseteq \mathcal{A}) \quad (42)$$

Note that  $f(a) - U_t(a) | H_t \sim \mathcal{N}(-\sqrt{\beta_t} \sigma_{t-1}(a), \sigma_{t-1}^2(a))$ . As in [12], by using that if  $X \sim \mathcal{N}(\mu, \sigma^2)$  for  $\mu \leq 0$ , then  $\mathbb{E}[(X)_+] \leq \frac{\sigma}{\sqrt{2\pi}} \exp\left(\frac{-\mu^2}{2\sigma^2}\right)$ , we get the following for  $R_1$ :

$$R_1 \leq \sum_{t \in [T]} \mathbb{E}_{H_t} \left[ \sum_{a \in \mathcal{A}} \mathbb{E}_t \left[ \frac{\sigma_{t-1}(a)}{\sqrt{2\pi}} \exp\left(\frac{-\beta_t}{2}\right) \middle| H_t \right] \right] \quad (43)$$

$$\leq \sum_{t \in [T]} \frac{|\mathcal{A}|}{\sqrt{2\pi}} \exp\left(\frac{-\beta_t}{2}\right) \quad (\sigma_{t-1}^2(a) \leq k(a, a) \leq 1) \quad (44)$$

$$\leq \sum_{t \in [T]} \frac{1}{t^2} \quad (\beta_t = 2 \log(|\mathcal{A}|t^2/\sqrt{2\pi})) \quad (45)$$

$$\leq \frac{\pi^2}{6} \quad \left( \sum_{t=1}^{\infty} \frac{1}{t^2} = \frac{\pi^2}{6} \right) \quad (46)$$

$\square$

**Lemma 8.**

$$\sum_{t \in [T]} \mathbb{E}[f(\mathbf{a}_t^*) - U_t(\mathbf{a}_t^*)] \leq \left( \frac{\sqrt{\pi}\omega}{\sqrt{2e(\omega-1)}} \right)^{1/\omega} \cdot \begin{cases} \frac{\omega}{\omega-\xi} T^{1-\frac{\xi}{\omega}} & \text{if } \xi/\omega < 1, \\ \frac{\xi}{\xi-\omega} & \text{if } \xi/\omega > 1. \end{cases} \quad (47)$$

*for Bayes-GP-UCB with confidence parameter  $\beta_t = 2(\text{erf}^{-1}(1-2\eta_t))^2$  and  $\eta_t = \frac{\sqrt{2\pi}\omega}{2|\mathcal{A}|^{\omega}t^\xi}$ ,  $\omega > 1$ .*

*Proof.* Following the proof of Lemma 7, we get that

$$\sum_{t \in [T]} \mathbb{E} [f(\mathbf{a}_t^*) - U_t(\mathbf{a}_t^*)] \leq \sum_{t \in [T]} \frac{|\mathcal{A}|}{\sqrt{2\pi}} \exp\left(-\frac{\beta_t}{2}\right). \quad (48)$$

Note that, according to Lemma 17,  $\text{erf}^{-1}(u) \geq \sqrt{-\omega^{-1} \log((1-u)/\vartheta)}$  for  $\omega > 1$  and  $\vartheta = \sqrt{2e/\pi} \sqrt{\omega-1}/\omega$ . We use the largest value of  $\vartheta$  permitted by Lemma 17 since it yields the tightest bound. Then,

$$\sum_{t \in [T]} \frac{|\mathcal{A}|}{\sqrt{2\pi}} \exp\left(-\frac{\beta_t}{2}\right) = \sum_{t \in [T]} \frac{|\mathcal{A}|}{\sqrt{2\pi}} \exp\left(-(\text{erf}^{-1}(1-2\eta_t))^2\right) \quad (49)$$

$$\leq \sum_{t \in [T]} \frac{|\mathcal{A}|}{\sqrt{2\pi}} \exp\left(\omega^{-1} \log\left(\frac{1-(1-2\eta_t)}{\vartheta}\right)\right) \quad (\text{Lemma 17}) \quad (50)$$

$$= \sum_{t \in [T]} \frac{|\mathcal{A}|}{\sqrt{2\pi}} \left(\frac{2\eta_t}{\vartheta}\right)^{\frac{1}{\omega}} \quad (51)$$

$$= \sum_{t \in [T]} \vartheta^{-\frac{1}{\omega}} t^{-\frac{\xi}{\omega}} \quad (\text{Definition of } \eta_t) \quad (52)$$

$$= \left(\frac{\sqrt{\pi}\omega}{\sqrt{2e(\omega-1)}}\right)^{\frac{1}{\omega}} \sum_{t \in [T]} t^{-\frac{\xi}{\omega}} \quad (\text{Definition of } \vartheta). \quad (53)$$

The behaviour of  $\sum_{t \in [T]} t^{-\frac{\xi}{\omega}}$  critically depends on the ratio  $\xi/\omega$ . If  $\xi/\omega < 1$ , then

$$\sum_{t \in [T]} t^{-\frac{\xi}{\omega}} \leq \int_0^T t^{-\frac{\xi}{\omega}} dt = T^{1-\frac{\xi}{\omega}} \frac{1}{1-\frac{\xi}{\omega}}. \quad (54)$$

On the other hand, if  $\xi/\omega > 1$ , then

$$\sum_{t \in [T]} t^{-\frac{\xi}{\omega}} \leq 1 + \int_1^\infty t^{-\frac{\xi}{\omega}} dt = 1 + \left[\frac{1}{1-\frac{\xi}{\omega}} t^{1-\frac{\xi}{\omega}}\right]_1^\infty = 1 - \frac{1}{1-\frac{\xi}{\omega}} = \frac{\xi}{\xi-\omega}. \quad (55)$$

□

Before we bound the right term in Lemma 6, we introduce a lemma for the confidence radius that applies to all the bandit algorithms considered.

**Lemma 9.**

$$\sum_{t \in [T]} \mathbb{E} \left[ \sum_{a \in \mathbf{a}_t} \sqrt{\beta_t} \sigma_{t-1}(a) \right] \leq \sqrt{C_4 T K \beta_T \gamma_{TK}} \quad (56)$$

where  $C_4 = 2/\log(1 + \varsigma^{-2})$  for GP-TS or any GP-UCB method with increasing confidence parameter  $\beta_t$ .

*Proof.*

$$\sum_{t \in [T]} \mathbb{E} \left[ \sum_{a \in \mathbf{a}_t} \sqrt{\beta_t} \sigma_{t-1}(a) \right] \quad (57)$$

$$= \mathbb{E} \left[ \sum_{t \in [T]} \sum_{a \in \mathbf{a}_t} \sqrt{\beta_t} \sigma_{t-1}(a) \right] \quad (58)$$

$$\leq \mathbb{E} \left[ \sqrt{\sum_{t \in [T]} \sum_{a \in \mathbf{a}_t} \beta_t} \sqrt{\sum_{t \in [T]} \sum_{a \in \mathbf{a}_t} \sigma_{t-1}^2(a)} \right] \quad (\text{Cauchy-Schwarz inequality}) \quad (59)$$

$$\leq \mathbb{E} \left[ \sqrt{TK\beta_T} \sqrt{\sum_{t \in [T]} \sum_{a \in \mathbf{a}_t} \sigma_{t-1}^2(a)} \right] \quad \left( |\mathbf{a}_t| \leq K, \max_{t \in [T]} \beta_t = \beta_T \right) \quad (60)$$

$$= \sqrt{TK\beta_T} \mathbb{E} \left[ \sqrt{\sum_{t \in [T]} \sum_{a \in \mathbf{a}_t} \sigma_{t-1}^2(a)} \right] \quad (61)$$

$$\leq \sqrt{TK\beta_T} \mathbb{E} \left[ \sqrt{C_4 \gamma_{TK}} \right]. \quad (\text{Lemma 5.4 from [11]}) \quad (62)$$

□

Next, we show how the right term in Lemma 6 can be rewritten in terms of the confidence radius for any GP-UCB method.

**Lemma 10.**

$$\sum_{t \in [T]} \mathbb{E} [U_t(\mathbf{a}_t) - f(\mathbf{a}_t)] = \sum_{t \in [T]} \mathbb{E} \left[ \sqrt{\beta_t} \sigma_{t-1}(\mathbf{a}_t) \right] \quad (63)$$

for any GP-UCB method with confidence parameter  $\beta_t$ .

*Proof.* Note that given the history  $H_t$ ,  $\mathbf{a}_t := \arg \max_{\mathbf{a} \in \mathcal{S}_t} U_t(\mathbf{a})$  is deterministic. Thus,

$$\sum_{t \in [T]} \mathbb{E} [U_t(\mathbf{a}_t) - f(\mathbf{a}_t)] = \sum_{t \in [T]} \mathbb{E}_{H_t} [\mathbb{E}_t [U_t(\mathbf{a}_t) - f(\mathbf{a}_t) | H_t]] \quad (64)$$

$$= \sum_{t \in [T]} \mathbb{E}_{H_t} \left[ \mathbb{E}_t \left[ \mu_{t-1}(\mathbf{a}_t) + \sqrt{\beta_t} \sigma_{t-1}(\mathbf{a}_t) - f(\mathbf{a}_t) \mid H_t \right] \right] \quad (65)$$

$$= \sum_{t \in [T]} \mathbb{E}_{H_t} \left[ \mathbb{E}_t \left[ \mu_{t-1}(\mathbf{a}_t) + \sqrt{\beta_t} \sigma_{t-1}(\mathbf{a}_t) - \mu_{t-1}(\mathbf{a}_t) \mid H_t \right] \right] \quad (66)$$

$$= \sum_{t \in [T]} \mathbb{E} \left[ \sqrt{\beta_t} \sigma_{t-1}(\mathbf{a}_t) \right] \quad (67)$$

□

For the final lemma in the finite case, we bound the right term in Lemma 6 for Thompson sampling using the previous results.

**Lemma 11.**

$$\sum_{t \in [T]} \mathbb{E} [U_t(\mathbf{a}_t) - f(\mathbf{a}_t)] \leq 2\sqrt{C_4 TK\beta_T \gamma_{TK}} + \frac{\pi^2}{6} \quad (68)$$

holds for GP-TS with  $\beta_t = 2 \log(|\mathcal{A}|t^2/\sqrt{2\pi})$ .

*Proof.* By adding and subtracting the lower bound  $L(\mathbf{a}_t)$ , we obtain

$$\sum_{t \in [T]} \mathbb{E} [U_t(\mathbf{a}_t) - f(\mathbf{a}_t)] = \sum_{t \in [T]} \mathbb{E} [U_t(\mathbf{a}_t) - f(\mathbf{a}_t) + L(\mathbf{a}_t) - L(\mathbf{a}_t)] \quad (69)$$

$$= \sum_{t \in [T]} \mathbb{E} [U_t(\mathbf{a}_t) - L(\mathbf{a}_t)] + \sum_{t \in [T]} \mathbb{E} [L(\mathbf{a}_t) - f(\mathbf{a}_t)] \quad (70)$$

$$= 2 \underbrace{\sum_{t \in [T]} \mathbb{E} \left[ \sqrt{\beta_t} \sigma_{t-1}(\mathbf{a}_t) \right]}_{(1)} + \underbrace{\sum_{t \in [T]} \mathbb{E} [L(\mathbf{a}_t) - f(\mathbf{a}_t)]}_{(2)}. \quad (71)$$

By Lemma 9, (1)  $\leq \sqrt{C_4TK\beta_T\gamma_{TK}}$ . The bound (2)  $\leq \frac{\pi^2}{6}$  is obtained using the same steps as in Lemma 7 due to the symmetry of  $L(\mathbf{a}_t) - f(\mathbf{a}_t)$  and  $f(\mathbf{a}_t) - U(\mathbf{a}_t)$ .  $\square$

Finally, we present and prove the regret bounds for GP-UCB, Bayes-GP-UCB and GP-TS using the established lemmas.

**Theorem 12** (Finite GP-UCB). *When  $\mathcal{A}$  is finite, the Bayesian regret of GP-UCB with  $\beta_t = 2 \log(|\mathcal{A}|t^2/\sqrt{2\pi})$  is bounded by:*

$$\text{BayesRegret}(T) \leq \frac{\pi^2}{6} + \sqrt{C_4TK\beta_T\gamma_{TK}} \quad (72)$$

where  $C_4 := 2/\log(1 + \varsigma^{-2})$ .

*Proof.*

$$\text{BayesRegret}(T) \leq \sum_{t \in [T]} \mathbb{E} [f(\mathbf{a}_t^*) - U_t(\mathbf{a}_t^*)] + \sum_{t \in [T]} \mathbb{E} [U_t(\mathbf{a}_t) - f(\mathbf{a}_t)] \quad (\text{Lemma 6}) \quad (73)$$

$$\leq \frac{\pi^2}{6} + \sum_{t \in [T]} \mathbb{E} \left[ \sqrt{\beta_t} \sigma_{t-1}(\mathbf{a}_t) \right] \quad (\text{Lemmas 7 and 10}) \quad (74)$$

$$\leq \frac{\pi^2}{6} + \sqrt{C_4TK\beta_T\gamma_{TK}}. \quad (\text{Lemma 9}) \quad (75)$$

$\square$

**Theorem 13** (Finite Bayes-GP-UCB). *When  $\mathcal{A}$  is finite, the Bayesian regret of Bayes-GP-UCB with  $\beta_t = 2(\text{erf}^{-1}(1 - 2\eta_t))^2$  for  $\eta_t = \frac{\sqrt{2\pi}\omega}{2|\mathcal{A}|^{\omega t^\xi}}$ ,  $\omega > 1$  is bounded by*

$$\text{BayesRegret}(T) \leq \sqrt{C_4TK\beta_T\gamma_{TK}} + \left( \frac{\sqrt{\pi}\omega}{\sqrt{2e(\omega - 1)}} \right)^{1/\omega} \cdot \begin{cases} \frac{\omega}{\omega - \xi} T^{1 - \frac{\xi}{\omega}} & \text{if } \xi/\omega < 1, \\ \frac{\xi}{\xi - \omega} & \text{if } \xi/\omega > 1. \end{cases} \quad (76)$$

*Proof.*

$$\text{BayesRegret}(T) \leq \sum_{t \in [T]} \mathbb{E} [U_t(\mathbf{a}_t) - f(\mathbf{a}_t)] + \sum_{t \in [T]} \mathbb{E} [f(\mathbf{a}_t^*) - U_t(\mathbf{a}_t^*)] \quad (\text{Lemma 6}) \quad (77)$$

$$\leq \sum_{t \in [T]} \mathbb{E} \left[ \sqrt{\beta_t} \sigma_{t-1}(\mathbf{a}_t) \right] \quad (\text{Lemma 10}) \quad (78)$$

$$+ \left( \frac{\sqrt{\pi}\omega}{\sqrt{2e(\omega - 1)}} \right)^{1/\omega} \cdot \begin{cases} \frac{\omega}{\omega - \xi} T^{1 - \frac{\xi}{\omega}} & \text{if } \xi/\omega < 1, \\ \frac{\xi}{\xi - \omega} & \text{if } \xi/\omega > 1. \end{cases} \quad (\text{Lemma 8}) \quad (79)$$

From Lemma 9,  $\sum_{t \in [T]} \mathbb{E} \left[ \sqrt{\beta_t} \sigma_{t-1}(\mathbf{a}_t) \right] \leq \sqrt{C_4TK\beta_T\gamma_{TK}}$  and we obtain the desired result.  $\square$

**Theorem 14** (Finite GP-TS). *When  $\mathcal{A}$  is finite, the Bayesian regret of GP-TS is bounded by:*

$$\text{BayesRegret}(T) \leq \frac{\pi^2}{3} + 2\sqrt{C_4TK\beta_T\gamma_{TK}} \quad (80)$$

where  $C_4 := 2/\log(1 + \varsigma^{-2})$  and  $\beta_t = 2 \log(|\mathcal{A}|t^2/\sqrt{2\pi})$ .



*Proof.*

$$\text{BayesRegret}(T) = \sum_{t \in [T]} \mathbb{E}[f(\mathbf{a}_t^*) - U_t(\mathbf{a}_t^*)] + \sum_{t \in [T]} \mathbb{E}[U_t(\mathbf{a}_t) - f(\mathbf{a}_t)] \quad (\text{Lemma 6}) \quad (81)$$

$$\leq \frac{\pi^2}{6} + \frac{\pi^2}{6} + 2\sqrt{C_4TK\beta_T\gamma_{TK}} \quad (\text{Lemmas 7 and 11}). \quad (82)$$

□

## B.2 Infinite case

Similar to the finite case, we establish lemmas that hold for all bandit algorithms and finally state and prove the regret bounds.

Before stating the first lemma, we restate the assumptions for convenience:

**Assumption 1** (Regularity assumptions). *Assume  $\mathcal{A} \subset [0, C_1]^d$  is a compact and convex set for some  $C_1 > 0$ . Furthermore, assume that  $\mu$  and  $k$  are both  $L$ -Lipschitz on  $\mathcal{A}$  and  $\mathcal{A} \times \mathcal{A}$ , respectively, for some  $L > 0$ . In addition, for  $f \sim \mathcal{GP}(\mu, k)$  assume that there exists constants  $C_2, C_3 > 0$  such that:*

$$\mathbb{P}\left(\sup_{a \in \mathcal{A}} \left| \frac{\partial f}{\partial a^{(j)}} \right| > l\right) \leq C_2 \exp\left(-\frac{l^2}{C_3^2}\right), \text{ for } j \in \{1, \dots, d\} \text{ and } l > 0 \quad (8)$$

where  $a^{(j)}$  denotes the  $j$ -th element of  $a$ .

**Assumption 2** (Discretization size). *Let  $\tau_t$  denote the number of discretization points per dimension and assume that*

$$\begin{cases} \tau_t \geq 2t^2KdC_1(1 + tK\varsigma^{-1}), \\ \tau_t/\beta_t \geq 8t^4K^2LdC_1, \\ \tau_t^2/\beta_t \geq 8t^5K^3L^2d^2C_1^2\varsigma^{-2}, \\ \tau_t \geq t^2KdC_1C_3\left(\sqrt{\log(C_2d)} + \frac{\sqrt{\pi}}{2}\right) \end{cases} \quad (9)$$

where the constants  $C_1, C_2, C_3$  and  $L$  are given by Assumption 1 whilst the constants  $d, K$  and  $\varsigma$  are defined by the bandit problem (Section 2.1).

**Remark 1.** *For the theorems to be relevant, the assumptions imposed on  $\tau_t$  must be satisfiable for some  $\tau_t$ . If  $\beta_t = 2 \log\left(\frac{\tau_t^d t^2}{\sqrt{2\pi}}\right)$ , then Assumption 2 is satisfied by*

$$\tau_t = \max \begin{cases} 2KdC_1(1 + tK\varsigma^{-1})t^2, \\ \left((16t^4K^2LdC_1)\left(d + \log\left(\frac{t^2}{\sqrt{2\pi}}\right)\right)\right)^{\frac{1}{1-1/e}}, \\ \left((16t^5K^3L^2d^2C_1^2\varsigma^{-2})\left(d + \log\left(\frac{t^2}{\sqrt{2\pi}}\right)\right)\right)^{\frac{1}{2-1/e}}, \\ t^2KdC_1C_3\left(\sqrt{\log(C_2d)} + \frac{\sqrt{\pi}}{2}\right). \end{cases} \quad (83)$$

This can be shown by noting that  $\log \tau_t \leq \sqrt[3]{\tau_t}$  and  $1 \leq \sqrt[3]{\tau_t}$  and then deriving that  $\frac{1}{\beta_t} \geq \frac{1}{\tau_t^{1/e}(d + \log(t^2/\sqrt{2\pi}))}$ .

Similarly, if  $\beta_t = 2(\text{erf}^{-1}(1 - 2\eta_t))^2$  and  $\eta_t = \frac{\sqrt{2\pi}^\omega}{2\tau_t^{d\omega} t^\xi}$ ,  $\omega > 1$ , then Assumption 2 is satisfied by

$$\tau_t = \max \begin{cases} 2t^2KdC_1(1 + tK\varsigma^{-1}), \\ \left((16t^4K^2LdC_1)\left(d\omega + \log\left(\frac{t^\xi}{2\sqrt{2\pi}^\omega}\right)\right)\right)^{\frac{1}{1-1/e}}, \\ \left((16t^5K^3L^2d^2C_1^2\varsigma^{-2})\left(d\omega + \log\left(\frac{t^\xi}{2\sqrt{2\pi}^\omega}\right)\right)\right)^{\frac{1}{2-1/e}}, \\ t^2KdC_1C_3\left(\sqrt{\log(C_2d)} + \frac{\sqrt{\pi}}{2}\right). \end{cases} \quad (84)$$

This is shown similarly as before but using Lemma 18 to upper bound  $\text{erf}^{-1}(1 - 2\eta_t)$  in  $\beta_t$ .

Next, we present a lemma that bounds the discretization error of the expected reward of optimal super arm.

**Lemma 15.** Let  $\mathcal{D}_t \subset \mathcal{A}$  be a finite discretization with each dimension equally divided into  $\tau_t = t^2 K d C_1 C_3 \left( \sqrt{\log(C_2 d)} + \sqrt{\pi/2} \right)$  such that  $|\mathcal{D}_t| = \tau_t^d$ . Then,

$$\sum_{t \in [T]} \mathbb{E} [f(\mathbf{a}_t^*) - f([\mathbf{a}_t^*]_{\mathcal{D}_t})] \leq \frac{\pi^2}{6}. \quad (85)$$

*Proof.*

$$\sum_{t \in [T]} \mathbb{E} [f(\mathbf{a}_t^*) - f([\mathbf{a}_t^*]_{\mathcal{D}_t})] = \sum_{t \in [T]} \mathbb{E} \left[ \sum_{a \in \mathbf{a}_t^*} f(a) - f([a]_{\mathcal{D}_t}) \right] \quad (86)$$

$$\leq K \sum_{t \in [T]} \mathbb{E} \left[ \sup_{a \in \mathcal{A}} f(a) - f([a]_{\mathcal{D}_t}) \right] \quad (|\mathbf{a}_t^*| \leq K) \quad (87)$$

$$\leq K \sum_{t \in [T]} \frac{1}{K t^2} \quad ([14, \text{Lemma H.2}] \text{ with } u_t = K t^2) \quad (88)$$

$$\leq \frac{\pi^2}{6} \quad \left( \sum_{t=1}^{\infty} \frac{1}{t^2} = \frac{\pi^2}{6} \right) \quad (89)$$

□

In the following lemma, we bound the discretization error of the posterior mean and standard deviation in terms of the regularity parameters, the discretization size and number of arms selected.

**Lemma 16.** Let  $\mu_{t-1}$  and  $\sigma_{t-1}$  denote the posterior mean and standard deviation of  $\mathcal{GP}(\mu, k)$  after sampling  $N_{t-1}$  base arms. If  $a \in \mathcal{A}$ , then

$$\mu_{t-1}([a]_{\mathcal{D}_t}) - \mu_{t-1}(a) \leq L \frac{dC_1}{\tau_t} + L \frac{dC_1}{\tau_t} \sqrt{N_{t-1} \varsigma^{-1} \sqrt{\|\mathbf{L}^{-1}(\mathbf{y} - \boldsymbol{\mu})\|_2^2}} \quad (90)$$

and

$$\sigma_{t-1}([a]_{\mathcal{D}_t}) - \sigma_{t-1}(a) \leq \sqrt{L \frac{dC_1}{\tau_t} + N_{t-1} L^2 \left( \frac{dC_1}{\tau_t} \right)^2 \varsigma^{-2}} \quad (91)$$

for  $L$ -Lipschitz  $\mu$  and  $k$  where  $\mathbf{L}$  is the Cholesky decomposition of  $\mathbf{K} + \varsigma^2 I$  and  $\|\mathbf{L}^{-1}(\mathbf{y} - \boldsymbol{\mu})\|_2^2 \sim \chi^2$  with  $N_{t-1}$  degrees of freedom.

*Proof.* Consider first the difference in posterior mean:

$$\mu_{t-1}([a]_{\mathcal{D}_t}) - \mu_{t-1}(a) \quad (92)$$

$$= \mu([a]_{\mathcal{D}_t}) - \mu(a) + (\mathbf{k}([a]_{\mathcal{D}_t}) - \mathbf{k}(a))^\top (\mathbf{K} + \varsigma^2 I)^{-1} (\mathbf{y} - \boldsymbol{\mu}) \quad (93)$$

$$\leq L \sup_{a \in \mathcal{A}} \|a - [a]_{\mathcal{D}_t}\|_1 + \left\| (\mathbf{k}([a]_{\mathcal{D}_t}) - \mathbf{k}(a))^\top (\mathbf{K} + \varsigma^2 I)^{-1} (\mathbf{y} - \boldsymbol{\mu}) \right\|_2 \quad (\mu \text{ } L\text{-Lipschitz}) \quad (94)$$

$$\leq L \frac{dr}{\tau_t} + \left\| (\mathbf{k}([a]_{\mathcal{D}_t}) - \mathbf{k}(a))^\top (\mathbf{K} + \varsigma^2 I)^{-1} (\mathbf{y} - \boldsymbol{\mu}) \right\|_2. \quad \left( \sup_{a \in \mathcal{A}} \|a - [a]_{\mathcal{D}_t}\| \leq \frac{dC_1}{\tau_t} \right) \quad (95)$$

Next, we will appropriately split the norm into a product of norms and bound the individual factors. Let  $\mathbf{K} + \varsigma^2 I = \mathbf{L}\mathbf{L}^\top$  denote the Cholesky decomposition. Note that  $\mathbf{y} - \boldsymbol{\mu} \sim \mathcal{N}(0, \mathbf{K} + \varsigma^2 I)$ . Then,  $\mathbf{L}^{-1}(\mathbf{y} - \boldsymbol{\mu}) \sim \mathcal{N}(0, \mathbf{L}^{-1}\mathbf{L}\mathbf{L}^\top(\mathbf{L}^{-1})^\top) = \mathcal{N}(0, I)$  and thus  $\|\mathbf{L}^{-1}(\mathbf{y} - \boldsymbol{\mu})\|_2$  has a chi distribution with  $N_{t-1}$  degrees of freedom.

Let  $\text{eig}(A)$  denote the set of eigenvalues of the square matrix  $A$ . The matrix norm of the inverted Cholesky decomposition  $\mathbf{L}^{-1}$  can be bounded as:

$$\|\mathbf{L}^{-1}\|_2 = \sqrt{\max \text{eig}((\mathbf{L}^{-1})^\top \mathbf{L}^{-1})} \quad ([58, \text{Eq. (538)}]) \quad (96)$$

$$= \sqrt{\max \text{eig}((\mathbf{K} + \varsigma^2 I)^{-1})} \quad (97)$$

$$= \sqrt{\max \frac{1}{\text{eig}(\mathbf{K} + \varsigma^2 I)}} \quad (98)$$

$$= \sqrt{\max \frac{1}{\text{eig}(\mathbf{K}) + \varsigma^2}} \leq \sqrt{\frac{1}{\varsigma^2}} \leq \frac{1}{\varsigma}. \quad (\mathbf{K} \text{ p.s.d.}, \varsigma > 0) \quad (99)$$

Similarly, we also get that

$$\|(\mathbf{K} + \varsigma^2 I)^{-1}\|_2 \leq \varsigma^{-2}. \quad (100)$$

The kernel difference can be bounded as follows:

$$\|\mathbf{k}([a]_{\mathcal{D}_t}) - \mathbf{k}(a)\|_2 = \sqrt{\sum_{i=1}^{N_{t-1}} (k([a]_{\mathcal{D}_t}, x_i) - k(a, x_i))^2} \quad (101)$$

$$\leq \sqrt{\sum_{i=1}^{N_{t-1}} L^2 \left(\frac{dr}{\tau_t}\right)^2} \leq L \frac{dr}{\tau_t} \sqrt{N_{t-1}} \quad (102)$$

where we use the fact that  $k$  is  $L$ -Lipschitz. Applying Cauchy-Schwarz and the obtained bounds, we find that

$$\mu_{t-1}([a]_{\mathcal{D}_t}) - \mu_{t-1}(a) \leq L \frac{dr}{\tau_t} + L \frac{dr}{\tau_t} \sqrt{N_{t-1}} \varsigma^{-1} \|\mathbf{L}^{-1}(\mathbf{y} - \boldsymbol{\mu})\|_2. \quad (103)$$

The posterior standard deviation is bounded similarly:

$$\sigma_{t-1}([a]_{\mathcal{D}_t}) - \sigma_{t-1}(a) \leq \sqrt{|\sigma_{t-1}^2([a]_{\mathcal{D}_t}) - \sigma_{t-1}^2(a)|}. \quad (104)$$

Continuing,

$$|\sigma_{t-1}^2([a]_{\mathcal{D}_t}) - \sigma_{t-1}^2(a)| \quad (105)$$

$$= |k([a]_{\mathcal{D}_t}, [a]_{\mathcal{D}_t}) - k(a, a)| \quad (106)$$

$$+ |(\mathbf{k}([a]_{\mathcal{D}_t}) - \mathbf{k}(a))^\top (\mathbf{K} + \varsigma^2 I)^{-1} (\mathbf{k}([a]_{\mathcal{D}_t}) - \mathbf{k}(a))| \quad (107)$$

$$\leq |k([a]_{\mathcal{D}_t}, [a]_{\mathcal{D}_t}) - k(a, a)| \quad (108)$$

$$+ |(\mathbf{k}([a]_{\mathcal{D}_t}) - \mathbf{k}(a))^\top (\mathbf{K} + \varsigma^2 I)^{-1} (\mathbf{k}([a]_{\mathcal{D}_t}) - \mathbf{k}(a))| \quad (109)$$

$$\leq L \frac{dr}{\tau_t} + \|\mathbf{k}([a]_{\mathcal{D}_t}) - \mathbf{k}(a)\|_2^2 \|(\mathbf{K} + \varsigma^2 I)^{-1}\|_2 \quad (110)$$

$$\leq L \frac{dr}{\tau_t} + \left(L \frac{dr}{\tau_t} \sqrt{N_{t-1}}\right)^2 \varsigma^{-2}. \quad (\text{Eqs. (100) and (102)}) \quad (111)$$

Combining the above, the final bound is:

$$\sigma_{t-1}([a]_{\mathcal{D}_t}) - \sigma_{t-1}(a) \leq \sqrt{L \frac{dC_1}{\tau_t} + N_{t-1} \left(L \frac{dC_2}{\tau_t}\right)^2} \varsigma^{-2}. \quad (112)$$

□

Using Lemma 16, we are ready to construct a constant bound for the expected discretization error of the posterior mean:

**Lemma 1.** *If Assumption 1 holds and  $\tau_t \geq 2t^2 K L d C_1 (1 + t K \varsigma^{-1})$ , then for any sequence of super arms  $\mathbf{a}_t \in \mathcal{S}_t$   $t \geq 1$ , the posterior mean  $\mu_{t-1}(\mathbf{a})$  satisfies*

$$\sum_{t \in [T]} \mathbb{E} [\mu_{t-1}([\mathbf{a}_t]_{\mathcal{D}_t}) - \mu_{t-1}(\mathbf{a}_t)] \leq \frac{\pi^2}{12}. \quad (10)$$

*Proof.* Note that the assumption on  $\tau_t$  is equivalent to  $KL \frac{dC_1}{\tau_t} (1+tK\zeta^{-1}) \leq \frac{1}{2t^2}$ . Then, we can bound the discretization error of the posterior mean as follows:

$$\sum_{t \in [T]} \mathbb{E} \left[ \sum_{a \in \mathbf{a}_t} \mu_{t-1}([a]_{\mathcal{D}_t}) - \mu_{t-1}(a) \right] \quad (113)$$

$$\leq \sum_{t \in [T]} \mathbb{E} \left[ K \sup_{a \in \mathcal{A}} [\mu_{t-1}([a]_{\mathcal{D}_t}) - \mu_{t-1}(a)] \right] \quad (|\mathbf{a}_t| \leq K) \quad (114)$$

$$\leq \sum_{t \in [T]} \mathbb{E} \left[ K \sup_{a \in \mathcal{A}} L \frac{dC_1}{\tau_t} \left( 1 + \sqrt{tK}\zeta^{-1} \sqrt{\|\mathbf{L}^{-1}(\mathbf{y} - \boldsymbol{\mu})\|_2^2} \right) \right] \quad (\text{Lemma 16 and } N_{t-1} < tK) \quad (115)$$

$$= \sum_{t \in [T]} \mathbb{E} \left[ KL \frac{dC_1}{\tau_t} \left( 1 + \sqrt{tK}\zeta^{-1} \sqrt{\|\mathbf{L}^{-1}(\mathbf{y} - \boldsymbol{\mu})\|_2^2} \right) \right] \quad (\mathbf{L}^{-1}, \mathbf{y}, \boldsymbol{\mu} \text{ independent of } a) \quad (116)$$

$$= \sum_{t \in [T]} KL \frac{dC_1}{\tau_t} \left( 1 + \sqrt{tK}\zeta^{-1} \mathbb{E} \left[ \sqrt{\|\mathbf{L}^{-1}(\mathbf{y} - \boldsymbol{\mu})\|_2^2} \right] \right) \quad (117)$$

$$\leq \sum_{t \in [T]} KL \frac{dC_1}{\tau_t} \left( 1 + \sqrt{tK}\zeta^{-1} \sqrt{\mathbb{E} [\|\mathbf{L}^{-1}(\mathbf{y} - \boldsymbol{\mu})\|_2^2]} \right) \quad (\text{Concave Jensen's inequality}) \quad (118)$$

$$= \sum_{t \in [T]} KL \frac{dC_1}{\tau_t} (1 + tK\zeta^{-1}) \quad \left( \|\mathbf{L}^{-1}(\mathbf{y} - \boldsymbol{\mu})\|_2^2 \sim \chi^2 \text{ with at} \right. \\ \left. \text{most } (t-1)K \text{ d.o.f.} \right) \quad (119)$$

$$\leq \sum_{t \in [T]} \frac{1}{2t^2} \quad (\text{Assumption on } \tau_t) \quad (120)$$

$$\leq \frac{\pi^2}{12}. \quad \left( \sum_{t=1}^{\infty} \frac{1}{t^2} = \frac{\pi^2}{6} \right) \quad (121)$$

See the proof of Lemma 16 for the motivation that  $\|\mathbf{L}^{-1}(\mathbf{y} - \boldsymbol{\mu})\|_2^2 \sim \chi^2$ .  $\square$

Similar to Lemma 1, we establish a constant bound for the discretization error of the posterior standard deviation:

**Lemma 2.** *If Assumption 1 holds and  $\tau_t$  satisfies*

$$\tau_t/\beta_t \geq 8t^4 K^2 L dC_1 \text{ and } \tau_t^2/\beta_t \geq 8t^5 K^3 L^2 d^2 C_1^2 \zeta^{-2} \quad (11)$$

*then, for any sequence of super arms  $\mathbf{a}_t \in \mathcal{S}_t$   $t \geq 1$ , the posterior standard deviation  $\sigma_{t-1}(\mathbf{a})$  satisfies*

$$\sum_{t \in [T]} \mathbb{E} \left[ \sqrt{\beta_t} (\sigma_{t-1}([\mathbf{a}_t]_{\mathcal{D}_t}) - \sigma_{t-1}(\mathbf{a}_t)) \right] \leq \frac{\pi^2}{12}. \quad (12)$$

*Proof.* Note that Eq. (11) is equivalent to

$$\beta_t K^2 L \frac{dC_1}{\tau_t} \leq \frac{1}{8t^4} \text{ and } \beta_t t K^3 L^2 \frac{d^2 C_1^2}{\tau_t^2} \zeta^{-2} \leq \frac{1}{8t^4}. \quad (122)$$

Then,

$$\sum_{t \in [T]} \mathbb{E} \left[ \sqrt{\beta_t} (\sigma_{t-1}([\mathbf{a}]_{\mathcal{D}_t}) - \sigma_{t-1}(\mathbf{a})) \right] \quad (123)$$

$$= \sum_{t \in [T]} \mathbb{E} \left[ \sum_{a \in \mathbf{a}} \sqrt{\beta_t} (\sigma_{t-1}([a]_{\mathcal{D}_t}) - \sigma_{t-1}(a)) \right] \quad (124)$$

$$\leq \sum_{t \in [T]} \mathbb{E} \left[ \sum_{a \in \mathbf{a}} \sqrt{\beta_t} \sqrt{L \frac{dC_1}{\tau_t} + tKL^2 \frac{d^2C_1^2}{\tau_t^2} \varsigma^{-2}} \right] \quad (\text{Lemma 16}) \quad (125)$$

$$\leq \sum_{t \in [T]} K \sqrt{\beta_t} \sqrt{L \frac{dC_1}{\tau_t} + tKL^2 \frac{d^2C_1^2}{\tau_t^2} \varsigma^{-2}} \quad (|\mathbf{a}| \leq K) \quad (126)$$

$$= \sum_{t \in [T]} \sqrt{\beta_t K^2 L \frac{dC_1}{\tau_t} + \beta_t t K^3 L^2 \frac{d^2C_1^2}{\tau_t^2} \varsigma^{-2}} \quad (127)$$

$$\leq \sum_{t \in [T]} \sqrt{\frac{1}{8t^4} + \frac{1}{8t^4}} \quad (\text{Eq. (122)}) \quad (128)$$

$$\leq \sum_{t \in [T]} \frac{1}{2t^2} \leq \frac{\pi^2}{12}. \quad \left( \sum_{t=1}^{\infty} \frac{1}{t^2} = \frac{\pi^2}{6} \right) \quad (129)$$

□

Finally, we are ready to prove the regret bounds for the infinite case:

**Theorem 3** (Infinite GP-UCB). *If Assumption 1 holds, then the Bayesian regret of GP-UCB with  $\beta_t = 2 \log(\tau_t^d t^2 / \sqrt{2\pi})$  is bounded by:*

$$\text{BayesRegret}(T) \leq \frac{\pi^2}{2} + \sqrt{C_4 T K \beta_T \gamma_{TK}} \quad (13)$$

where  $\tau_t$  satisfies Assumption 2 and  $C_4 = 2 / \log(1 + \varsigma^{-2})$ .

*Proof.* Similar to [14, 11], we use a fixed discretization  $\mathcal{D}_t \subset \mathcal{A}$  for  $t \geq 1$ . Let  $\mathcal{D}_t \subset \mathcal{A}$  be a finite set with  $|\mathcal{D}_t| = \tau_t^d$  and each dimension equally divided into  $\tau_t$  points with  $\tau_t$  satisfying Assumption 1. Let  $[a]_{\mathcal{D}_t}$  denote the nearest point in  $\mathcal{D}_t$  for  $a \in \mathcal{A}$  and similarly let  $[\mathbf{a}]_{\mathcal{D}_t} = \{[a]_{\mathcal{D}_t} | a \in \mathbf{a}\}$  for  $\mathbf{a} \subset \mathcal{A}$ .

As in [14], we decompose the Bayesian regret into several parts:

$$\text{BayesRegret}(T) = \sum_{t \in [T]} \mathbb{E} \left[ \underbrace{f(\mathbf{a}_t^*) - f([\mathbf{a}_t^*]_{\mathcal{D}_t})}_{(1)} + \underbrace{f([\mathbf{a}_t^*]_{\mathcal{D}_t}) - U_t([\mathbf{a}_t^*]_{\mathcal{D}_t})}_{(2)} \right] \quad (130)$$

$$+ \underbrace{U_t([\mathbf{a}_t^*]_{\mathcal{D}_t}) - U_t(\mathbf{a}_t^*)}_{(3)} + \underbrace{U_t(\mathbf{a}_t^*) - U_t(\mathbf{a}_t)}_{(4)} \quad (131)$$

$$+ \underbrace{U_t(\mathbf{a}_t) - f(\mathbf{a}_t)}_{(5)} \quad (132)$$

Term (1) can be bounded using Lemma 15:  $\sum_{t \in [T]} \mathbb{E}[f(\mathbf{a}_t^*) - f([\mathbf{a}_t^*]_{\mathcal{D}_t})] \leq \frac{\pi^2}{6}$ . Terms (2) and (5) can be bounded using the finite case with  $\beta_t = 2 \log(|\mathcal{D}_t| t^2 / \sqrt{2\pi})$ . Then,

$$\sum_{t \in [T]} \mathbb{E}[f([\mathbf{a}_t^*]_{\mathcal{D}_t}) - U_t([\mathbf{a}_t^*]_{\mathcal{D}_t}) + U_t(\mathbf{a}_t) - f(\mathbf{a}_t)] \leq \frac{\pi^2}{6} + \sqrt{C_4 T K \beta_T \gamma_{TK}}. \quad (\text{Lemmas 7, 9 and 10}) \quad (133)$$

Takeno et al. considers the term  $U_t([\mathbf{a}_t^*]_{\mathcal{D}_t}) - U_t(\mathbf{a}_t^*)$  and argues that it is non-positive since  $\mathbf{a}_t = \arg \max_{\mathbf{a} \in \mathcal{S}_t} U_t(\mathbf{a})$ . Unlike [14], we do not assume that all arms are available at time  $t$  and thus  $[\mathbf{a}_t^*]_{\mathcal{D}_t} \in \mathcal{S}_t$  does not necessarily hold. By further decomposing this term into (3) and (4), the same argument can be applied to term (4):  $U_t(\mathbf{a}_t^*) - U_t(\mathbf{a}_t) \leq 0$ . Then, term (3) can be bounded using Lemmas 1 and 2:

$$\sum_{t \in [T]} \mathbb{E}[(3)] = \sum_{t \in [T]} \mathbb{E} \left[ \mu_{t-1}([\mathbf{a}_t^*]_{\mathcal{D}_t}) - \mu_{t-1}(\mathbf{a}_t^*) + \sqrt{\beta_t} (\sigma_{t-1}([\mathbf{a}_t^*]_{\mathcal{D}_t}) - \sigma_{t-1}(\mathbf{a}_t^*)) \right] \quad (134)$$

$$\leq \frac{\pi^2}{12} + \frac{\pi^2}{12}. \quad (\text{Lemmas 1 and 2}) \quad (135)$$

Finally, by combining the bounds for all terms we get that

$$\text{BayesRegret}(T) \leq \frac{\pi^2}{2} + \sqrt{C_4 T K \beta_T \gamma_{TK}}. \quad (136)$$

□

**Theorem 4** (Infinite Bayes-GP-UCB). *If Assumption 1 holds, then the Bayesian regret of Bayes-GP-UCB with  $\beta_t = 2 (\text{erf}^{-1}(1 - 2\eta_t))^2$  for  $\eta_t = (2\pi)^{\omega/2} / (2\tau_t^{d\omega} t^\gamma)$ ,  $\omega > 1$  is bounded by:*

$$\text{BayesRegret}(T) \leq \frac{\pi^2}{3} + \sqrt{C_4 T K \beta_T \gamma_{TK}} + \left( \frac{\sqrt{\pi\omega}}{\sqrt{2e(\omega-1)}} \right)^{1/\omega} \begin{cases} \frac{\omega}{\omega-\xi} T^{1-\frac{\xi}{\omega}} & \text{if } \xi/\omega < 1, \\ \frac{\xi}{\xi-\omega} & \text{if } \xi/\omega > 1. \end{cases} \quad (14)$$

where  $\tau_t$  satisfies Assumption 2 and  $C_4 = 2/\log(1 + \varsigma^{-2})$ .

*Proof.* Can be shown by following the steps of Theorem 3 and using the finite case for Bayes-GP-UCB (Theorem 13). □

**Theorem 5** (Infinite GP-TS). *If Assumption 1 holds, then the Bayesian regret of GP-TS is bounded by:*

$$\text{BayesRegret}(T) \leq \frac{2\pi^2}{3} + 2\sqrt{C_4 T K \beta_T \gamma_{TK}} \quad (15)$$

where  $\beta_t = 2 \log(\tau_t^{dt^2} / \sqrt{2\pi})$  with  $\tau_t$  satisfying Assumption 2 and  $C_4 = 2/\log(1 + \varsigma^{-2})$ .

*Proof.* As in the proof of Theorem 3, assume that we have a discretization  $\mathcal{D}_t$  and decompose the Bayesian regret into 4 terms:

$$\text{BayesRegret}(T) = \sum_{t \in [T]} \mathbb{E} \left[ \underbrace{f(\mathbf{a}_t^*) - f([\mathbf{a}_t^*]_{\mathcal{D}_t})}_{(1)} + \underbrace{f([\mathbf{a}_t^*]_{\mathcal{D}_t}) - U_t([\mathbf{a}_t^*]_{\mathcal{D}_t})}_{(2)} \right] \quad (137)$$

$$+ \underbrace{U_t([\mathbf{a}_t^*]_{\mathcal{D}_t}) - U_t(\mathbf{a}_t)}_{(3)} + \underbrace{U_t(\mathbf{a}_t) - f(\mathbf{a}_t)}_{(4)}. \quad (138)$$

As in the proof of Theorem 3, term (1) is dealt with using Lemma 15 and term (2) and (4) are handled as in the finite case (Theorem 14):

$$\sum_{t \in [T]} \mathbb{E}[(1) + (2) + (3)] \leq \frac{\pi^2}{6} + \frac{\pi^2}{3} + 2\sqrt{C_4 T K \beta_T \gamma_{TK}}. \quad (139)$$

To bound term (3), we start by utilizing that  $\mathbf{a}_t^* | H_t \stackrel{d}{=} \mathbf{a}_t | H_t$  and  $U_t([\cdot]_{\mathcal{D}_t}) | H_t$  is deterministic and thus:

$$\sum_{t \in [T]} \mathbb{E}[(3)] = \sum_{t \in [T]} \mathbb{E}_{H_t} [\mathbb{E}_t [U_t([\mathbf{a}_t^*]_{\mathcal{D}_t}) - U_t(\mathbf{a}_t) | H_t]] \quad (140)$$

$$= \sum_{t \in [T]} \mathbb{E}_{H_t} [\mathbb{E}_t [U_t([\mathbf{a}_t]_{\mathcal{D}_t}) - U_t(\mathbf{a}_t) | H_t]] \quad (141)$$

$$= \sum_{t \in [T]} \mathbb{E} \left[ \mu_{t-1}([\mathbf{a}_t]_{\mathcal{D}_t}) - \mu_{t-1}(\mathbf{a}_t) + \sqrt{\beta_t} (\sigma_{t-1}([\mathbf{a}_t]_{\mathcal{D}_t}) - \sigma_{t-1}(\mathbf{a}_t)) \right] \quad (142)$$

$$\leq \frac{\pi^2}{12} + \frac{\pi^2}{12}. \quad (\text{Lemmas 1 and 2}) \quad (143)$$

Put together, we have that

$$\text{BayesRegret}(T) \leq \frac{2\pi^2}{3} + 2\sqrt{C_4 T K \beta_T \gamma_{TK}}. \quad (144)$$

□

### B.3 Additional lemmas for inverse error function

**Lemma 17.** *The inverse error function is lower bounded by*

$$\operatorname{erf}^{-1}(u) \geq \sqrt{-\omega^{-1} \log \left( \frac{1-u}{\vartheta} \right)} \quad (145)$$

for  $u \in [0, 1)$ ,  $\omega > 1$  and  $0 < \vartheta \leq \sqrt{\frac{2e}{\pi} \frac{\sqrt{\omega-1}}{\omega}}$ .

*Proof.* According to Theorem 2 of [35],  $\operatorname{erfc}(u) \geq \vartheta \exp(-\omega u^2)$  for  $\omega > 1$  and  $0 < \vartheta \leq \sqrt{\frac{2e}{\pi} \frac{\sqrt{\omega-1}}{\omega}}$ . Since  $\operatorname{erf}(u) = 1 - \operatorname{erfc}(u)$ , it follows that  $\operatorname{erf}(u) \leq 1 - \vartheta \exp(-\omega u^2) =: h(u)$ .

In general, if  $f(x) \leq g(x)$  then  $f^{-1}(x) \geq g^{-1}(x)$ . Thus,  $\operatorname{erf}^{-1}(u) \geq h^{-1}(u) = \sqrt{-\omega^{-1} \log \left( \frac{1-u}{\vartheta} \right)}$ .  $\square$

**Lemma 18.** *The inverse error function is upper bounded by*

$$\operatorname{erf}^{-1}(u) \leq \sqrt{-\omega^{-1} \log \left( \frac{1-u}{\vartheta} \right)} \quad (146)$$

for  $u \in [0, 1)$ ,  $\vartheta \geq 1$  and  $0 < \omega \leq 1$ .

*Proof.* The same arguments as in Lemma 17 but using Theorem 1 of [35].  $\square$